

ALMA MATER STUDIORUM · UNIVERSITÀ DI
BOLOGNA

SCUOLA DI SCIENZE

Corso di Laurea Magistrale in Matematica

Laplace Operator on Finite Graphs
and
a Network Diffusion Model for the
Progression of the Alzheimer Disease

Tesi di Laurea in Analisi Matematica

Relatore:
Chiar.mo Prof.
Bruno Franchi

Presentata da:
Veronica Tora

‡ II Sessione
Anno Accademico 2013-2014

*Alla curiosità,
agli orizzonti possibili e
al profumo della ginestra
che fiorisce nei deserti*

...

Introduction

Alzheimer is the most common form of dementia and it is estimated to affect 25 million of people over 65 years of age worldwide. The effective causes of the disease and the mechanisms of progression are not known exactly and are an actual topic of scientific research. An interesting hypothesis well-supported by several studies on neurodegeneration is that the disease is transmitted by " prion-like" mechanism : misfolded proteins can induce other proteins of the same type to assume the pathological conformation. In this sense Alzheimer is a misfolding protein disease. Recent findings on neurodegenerative diseases allow us to extend the previous considerations to all forms of dementia, stating the hypothesis that although dementias have different causes and origins, they might share a common mechanism of transmission. This is the point of depart of the research of A. Ray, A. Kuceyeski, M. Weiner published in the journal *Neuron* (2012), that we will present in this thesis. We thank professor A. Ray for giving the permission to use the figures of his paper.

In this study, in order to describe the progression of dementia, a *Network Diffusion Model* is built; a general "disease factor" is identified and its progression through the "healthy brain" according to a diffusion mechanism depending on concentration gradients is analyzed. Moreover the healthy brain is approximated by a "network" (said "healthy brain network") that is, in mathematical terms, a weighted graph in which each vertex represents a region of interest while the connections between them are described by the edges. These considerations explain why the name "network diffusion model"

is given.

The "heat equation" on the graph is derived to analyze the behaviour of the disease factor. We have an explicit formula for the solution of this equation, that depends on the eigenfunctions of the Laplace operator of the graph and in this model represents how the disease factor spreads through the network. From a macroscopic point of view the disease gives rise to a loss of neurons and synapsis in the cerebral cortex and in some subcortical regions with the consequent reduction of the volume and "wasting away" of the affected areas. This process is said "atrophy" and it is described through a function depending on time. In Network Diffusion Model atrophy in a determined brain region is supposed to be the accumulation of the disease factor in that area, therefore by integration of the disease factor in the whole healthy brain network on a certain time interval atrophy patterns on brain are obtained. The core of the model is that the function describing atrophy depends significantly on the eigenvalues and the eigenfunctions of the Laplacian of the graph and for times of interest only a small number of eigenfunctions contributes in the increasing of atrophy. This suggests the possibility of a strong relationship between this small number of eigenfunctions and atrophy.

MRI scans of 14 young subjects and 18 AD, 18 bvFTD (behavioral variant frontotemporal dementia), 19 age-matched normal subjects are achieved in order to provide an experimental basis for the model. The former are used to build the healthy brain network, while the latter are achieved in order to measure effective atrophy patterns of disease. As the eigenfunctions of the Laplacian of a graph are fuctions on the set of the vertices of the graph, the eigenfunctions significant for the progression of atropy are calculated and their values on each vertex of the network are compared (through visual corrispondence and statistical analysis) with the amount of atrophy measured for each form of dementia (considered in the dataset) in the cerebral area corresponding to that vertex. Strong agreement is observed between experimental analysis and theoretical results. In particular the second eigenfunction closely resembles atrophy patterns of Alzheimer disease while the

third eigenfunction is a good representation of atrophy patterns of bvFTD. In the rest of the thesis we describe the mathematical background and objects used in the model. An overview on finite graphs is shown. The Laplace operator for finite graphs is presented, before for unweighted graphs and then for weighted graphs. Eigenvalues upper and lower bounds for graphs are derived. In order to provide a complete mathematical framework the relationship between discrete and continuous case is described. Laplace-Beltrami operator on compact Riemannian manifolds is presented and eigenvalues upper bounds for manifolds are derived starting from eigenvalues upper bounds for finite graphs.

Introduzione

La malattia di Alzheimer è la più comune forma di demenza senile e affligge secondo recenti stime più di 25 milioni di persone nel mondo sopra i 65 anni di età. Le effettive cause e i meccanismi di progressione della malattia non sono noti nella loro interezza e sono attualmente oggetto di ricerca scientifica. Un'ipotesi interessante, ampiamente supportata da ricerche sui processi neurodegenerativi, consiste nel considerare il meccanismo di progressione della malattia come se fosse simile a un' infezione da prioni: alcune specifiche proteine durante il loro processo di assemblaggio assumono una conformazione patologica dovuta a uno scorretto ripiegamento proteico (ovvero la fase in cui la proteina acquisisce la sua forma tridimensionale). Tali proteine inducono altre proteine dello stesso tipo ad assumere la suddetta conformazione patologica.

Da quanto si evince da recenti studi sulle malattie neurodegenerative è possibile estendere le precedenti considerazioni a tutte le forme di demenza, avanzando l'ipotesi che sebbene le varie tipologie di demenze senili abbiano differenti cause e origini si possa individuare un comune meccanismo di evoluzione. Questo è il punto di partenza della ricerca di A. Ray, A. Kuceyeski, M. Weiner pubblicata nella rivista *Neuron* (2012), che presenteremo nella tesi. Si ringrazia, a tale proposito, il professor A. Ray per la concessione dell'uso delle immagini presenti nel suo lavoro.

In tale ricerca, la progressione della demenza senile viene descritta mediante la costruzione del modello *Network Diffusion Model*; l'identificazione di un generale "fattore di malattia" è seguita dall'analisi della sua progressione

nelle regioni cerebrali secondo meccanismi diffusivi dipendenti dai gradienti di concentrazione dello stesso fattore di malattia. "L'encefalo sano" viene approssimato con una "rete cerebrale" ovvero con un grafo in cui ciascun vertice rappresenta una regione cerebrale di interesse mentre le connessioni tra queste ultime sono descritte dagli spigoli del grafo. Per tali ragioni il modello è stato chiamato *Network Diffusion Model*. Al fine di analizzare il comportamento del "fattore di malattia" si utilizza l'equazione del calore sul grafo. Quest'ultima è risolvibile esplicitamente e la soluzione, che rappresenta come il fattore di malattia si diffonda nella rete cerebrale, dipende dalle autofunzioni dell'operatore di Laplace sul grafo.

Da un punto di vista macroscopico la malattia dà luogo a una perdita di neuroni e sinapsi nella corteccia cerebrale e in alcune regioni subcorticali con la conseguente riduzione di volume e deterioramento delle aree contigue. Tale processo è detto atrofia e viene descritto mediante una funzione dipendente dal tempo. Inoltre, nel modello preso in esame si suppone che l'atrofia in una determinata regione cerebrale sia data dall' "accumulo" (o dalla quantità) del fattore di malattia in quella stessa area; dunque, integrando il fattore di malattia sull'intera rete cerebrale in un certo intervallo di tempo, si ottiene un'espressione per atrofia nell'intero encefalo in quell'intervallo. Si osserva che la funzione che descrive l'atrofia dipende significativamente dagli autovalori e dalle autofunzioni del Laplaciano del grafo e per tempi di interesse solo un piccolo numero di autofunzioni contribuisce all'aumento dell'atrofia. Ciò suggerisce la possibilità di un forte legame tra questo piccolo numero di autofunzioni e l'atrofia.

Quattordici giovani volontari, diciotto pazienti affetti da Alzheimer (AD), diciotto pazienti affetti da variante comportamentale della demenza frontotemporale (bvFTD) e diciannove anziani sani vengono sottoposti alla risonanza magnetica in modo da costruire una base sperimentale per il modello. Dalla risonanza magnetica dei quattordici giovani si ottengono gli strumenti per costruire la "rete cerebrale sana", mentre le restanti vengono utilizzate per misurare l'atrofia effettiva associata alle diverse malattie. Dato che le

autofunzioni del laplaciano sono funzioni sull'insieme dei vertici del grafo, si calcolano le autofunzioni significative per l' aumento dell'atrofia e si confrontano (tramite corrispondenza visiva e analisi statistica) i loro valori su ogni vertice della rete con la "quantità di atrofia misurata per ogni forma di demenza (considerata nel dataset) nell'area cerebrale corrispondente a quel vertice.

L'analisi sperimentale concorda fortemente con i risultati teorici. In particolare, i valori della seconda autofunzione su ogni vertice della rete rispecchiano la quantità di atrofia rilevata nel morbo di Alzheimer, mentre la terza autofunzione è una buona rappresentazione per l'atrofia misurata in pazienti affetti da bvFTD.

Nel resto della tesi vengono descritti il contesto e gli oggetti matematici utilizzati nel modello: viene presentata una panoramica sui grafi finiti; in seguito viene introdotto l'operatore di Laplace, prima per grafi non pesati e poi per grafi pesati, e si forniscono stime dall'alto e dal basso per gli autovalori. Al fine di costruire una cornice matematica completa si analizza la relazione tra caso discreto e continuo: viene descritto l'operatore di Laplace-Beltrami sulle varietà riemanniane compatte e vengono fornite stime dall'alto per gli autovalori dell'operatore di Laplace-Beltrami associato a tali varietà a partire dalle stime dall'alto per gli autovalori del laplaciano sui grafi finiti.

Contents

Introduction	i
Introduzione	v
1 The Laplace operator for graphs	1
1.1 Generalities about graphs	1
1.2 Eigenvalues and Laplacian of a graph	5
1.3 Eigenvalues upper and lower bounds for graphs	8
1.4 The Laplacian of a weighted graph	14
2 From graphs to manifolds: relationship between discrete and continuous case	17
2.1 Eigenvalues and diameter of a graph	17
2.2 Eigenvalues upper bounds for manifolds	21
3 The Alzheimer's disease and other Dementias	33
3.1 Generalities about Dementia	33
3.2 Overview on findings about dementias' causes and progression mechanisms	36
4 The Network Diffusion Model	43
4.1 Processing steps of the network diffusion model	43
4.2 The network heat equation	44
4.3 Dynamics evolution of cortical atrophy	51
4.4 The role of the eigenmodes in Network Diffusion Model	53

4.5	Medical and diagnostic implications of the model	58
5	Appendix	61
5.1	The calculus of the exponential matrix	61
5.2	The structure of solutions of homogeneous linear systems of EDO	65
	Bibliography	69

List of Figures

1.1	Example of complete graph of 5 vertices i.e. a 4-regular graph	3
1.2	Example of connected graph	4
1.3	Example of bipartite graph	4
1.4	Example of weighted graph	15
3.1	Comparison between an healthy brain and a brain affected by Alzheimer's disease	35
3.2	Formation of Beta-Amyloid plaques	38
3.3	Disintegration of microtubules in brain cells due to misfolded tau protein	39
3.4	Heterodimer model of prion replication mechanism: a single $\text{Pr}P^{Sc}$ molecule binds to a single $\text{Pr}P^C$ molecule and catalyzes its conversion into $\text{Pr}P^{Sc}$. The two $\text{Pr}P^{Sc}$ molecules then come apart and can go on to convert more $\text{Pr}P^C$	40
3.5	Fibril model of prion replication mechanism: it starts from the assumption that $\text{Pr}P^{Sc}$ exists only as fibrils. Fibril ends bind $\text{Pr}P^C$ and convert it into $\text{Pr}P^{Sc}$	41

-
- 4.1 Diagram of the processing steps of the Network Diffusion Model: (left) "Healthy brain network" is obtained by MRI scans of 14 young volunteers followed by whole brain tractography. Cortical and subcortical gray matter regions are represented by nodes of the network, while the number and the strength of fiber tracts that connect them are described by the edges of the network. Proposed network diffusion model and its eigenmodes are derived from this healthy network. Predicted atrophy patterns are plotted. (right) Measurement of atrophy patterns of AD and bvFTD patients. Volume of each cortical and subcortical grey matter region is measured. Atrophy of each region is estimated through a statistic of interest between the diseased and the age-matched normal groups. The results are plotted and compared with predicted atrophy patterns. 45
- 4.2 Visual correspondence between theoretical prediction and measured Alzheimer's atrophy patterns: Wire-and-ball plot represent whole brain atrophy patterns, where each brain region of interest is depicted as a ball whose size is proportional to the atrophy level in that area. The color of the ball denotes the lobe of interest: blues stands for frontal lobe, purple parietal lobe, green occipital lobe, red temporal lobe and cyan subcortical region.(Top) Theoretical prediction of atrophy is based on the second eigenmode of the young healthy brain network's Laplacian matrix H . The second eigenmode evaluated at each region of interest is represented by the size of the corresponding ball.(Bottom) Measured atrophy patterns obtained by 18 AD patients are represented. We observe strong correspondence between predicted and measured atrophy. 55

- 4.3 Visual correspondence between theoretical prediction and measured bvFTD's atrophy patterns:(Top) Theoretical prediction of atrophy is based on the third eigenmode of the young healthy brain network's Laplacian matrix H . The value of the third eigenmode at each region of interest is represented by the size of the corresponding ball.(Bottom) Atrophy patterns measured in brain region of interest obtained by 18 bvFTD patients are represented by the size of the corresponding ball. We observe strong resemblance between predicted and measured atrophy. 56
- 4.4 Correlations between Measured Atrophy of AD/bvFTD versus Predicted Atrophy from the First Three Eigenmodes of the Young Healthy Network: The x axis in each panel represents a measured level of atrophy through a statistic of interest (bottom). The y axes are eigenmodes of the healthy network: u_1 (left column), u_2 (middle column), and u_3 (right column). Each dot in the plots corresponds to a single grey matter region. Different colors of dots stand for different lobes. A line of best fit is also shown in each panel. Correlations within diagonally located panels are high, and correlations in off-diagonal panels are low. Most significant plots are indicated by green boxes, and they are along the diagonal panels. High correspondence between eigenmodes and dementia atrophy is shown. 57

Chapter 1

The Laplace operator for graphs

1.1 Generalities about graphs

A finite graph is a representation of a finite set of objects where some pairs of objects are connected by links. The objects are called vertices, while the links are said edges. We usually depict a graph as a set of dots for the vertices, joined by lines or curves for the edges. We will deal with undirect graphs, that are graphs whose edges have no orientation.

In mathematical terms, we are able to give the following definition:

Definition 1.1. A graph G is an ordered pair of disjoint sets $(V(G), E(G))$, where $V(G) = \{v_1, \dots, v_n\}$ denotes the set of the vertex of the graph G while $E(G)$ is the set of the unordered pairs

$$\{\{v_i, v_j\} \text{ such that the vertex } v_i \text{ is linked to the vertex } v_j\}$$

and denotes the set of the edges of G

We observe that $V(G)$ and $E(G)$ are taken to be finite and this is the case that we will analyze. Many of the well-known results fail in the infinite case.

Definition 1.2. The number of vertices of a graph is said order and it is expressed by $|V|$, while $|E|$ is the graph's size and represents the number of edges.

Definition 1.3. Let d_{v_i} denote the degree of the vertex v_i that is given by the number of edges that connect to it, while an edge that connects to the vertex at both ends is said loop.

Definition 1.4. If $d_{v_i} = 0$, v_i is said isolated vertex.

A graph that has at least one edge is said non trivial.

Definition 1.5. We say that $G' = (V', E')$ is a subgraph of $G = (V, E)$ if $V' \subset V$ and $E' \subset E$. A subgraph is said maximal if for any of its vertices the all edges that connect to it belong to the subgraph.

A basic relation in graph theory is the following:

Definition 1.6. If $\{v_i, v_j\} \in E(G)$, v_i, v_j are said adjacent vertices of G . In symbols: $v_i \sim v_j$. The adjacency is a symmetric binary relation.

Definition 1.7. The following matrix:

$$A := a_{i,j} = \begin{cases} 1 & \text{if } v_i \text{ and } v_j \text{ are adjacent} \\ 0 & \text{otherwise} \end{cases} \quad (1.1)$$

is said the adjacency matrix of the graph.

There are several graph classes. In our discussion we will treat with the following :

Definition 1.8. A graph is said regular if each vertex has the same number of edges that connect to it, i.e. $d_{v_i} = \text{constant } \forall v_i$. A regular graph with vertices of degree k is called a k -regular graph.

Definition 1.9. A graph is said complete if each pair of vertices is connected by an edge.

Remark 1. Complete graphs of n vertices are all isomorphic. It means that for each pair of complete graphs D, H there exists a bijection between the vertex sets of D and H

$$f : V(D) \rightarrow V(H)$$

such that any two vertices v_i, v_j are adjacent in D if and only if $f(v_i)$ and $f(v_j)$ are adjacent in H . The graph isomorphism is an equivalence relation on graphs and a set of graphs isomorphic to each other is said an isomorphism class of graphs.

We denote by K_n the n -th isomorphism class for complete graphs. Each graph that belongs to the class k_n has $\frac{n(n-1)}{2}$ edges and in particular is a $n - 1$ regular graph.

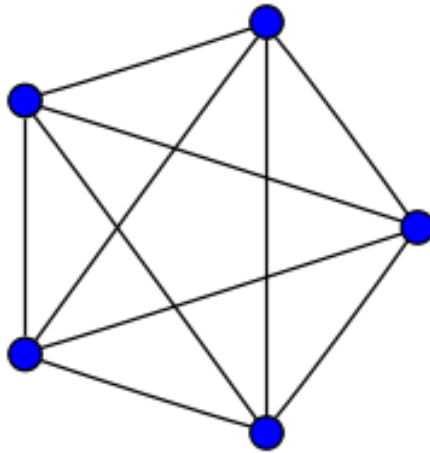


Figure 1.1: Example of complete graph of 5 vertices i.e. a 4-regular graph

Definition 1.10. Connected graphs have the feature that for each pair of vertices v_i, v_j there is a path joining them. A connected component of a graph is a maximal connected subgraph.

Definition 1.11. A graph is said bipartite if the vertex set can be partitioned into two subsets X, Y with the feature that in both the subsets there is not any pair of adjacent vertices.

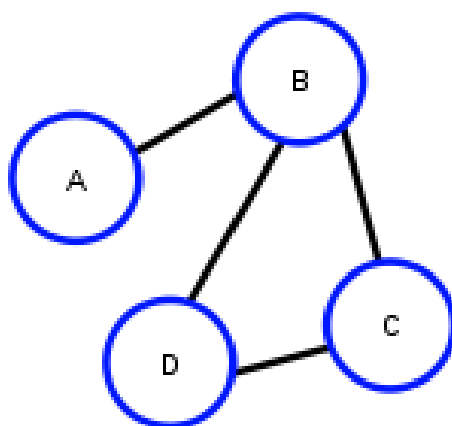


Figure 1.2: Example of connected graph

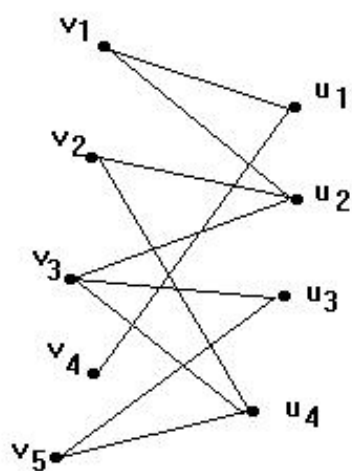


Figure 1.3: Example of bipartite graph

1.2 Eigenvalues and Laplacian of a graph

In a finite graph G , let $\{v_1, \dots, v_n\}$ denote the set of the vertices and d_{v_i} $i = 1, \dots, n$ denote the degree of the corresponding vertex. In order to define the Laplacian for a graph without loops or multiple edges, we consider the $n \times n$ matrix with rows and columns indexed by the vertices of G :

$$L := l_{i,j} \begin{cases} d_{v_i} & \text{if } v_i = v_j \\ -1 & \text{if } v_i \text{ and } v_j \text{ are adjacent} \\ 0 & \text{otherwise} \end{cases} \quad (1.2)$$

Definition 1.12. The following matrix is said Laplacian of the graph G :

$$\mathbf{L} := \mathbf{l}_{i,j} = \begin{cases} 1 & \text{if } i = j \\ \frac{-1}{\sqrt{d_{v_i}d_{v_j}}} & \text{if } v_i \text{ and } v_j \text{ are adjacent} \\ 0 & \text{otherwise} \end{cases} \quad (1.3)$$

with $i, j = 1, \dots, n$.

Let T denote the diagonal matrix with the (i, i) -th entry having the value d_{v_i} . The Laplacian of G can be expressed by the formula:

$$\mathbf{L} = T^{-\frac{1}{2}} L T^{-\frac{1}{2}}$$

with the convention $T_{i,i}^{-1} = 0$ for $d_{v_i} = 0$. The Laplacian of a k -regular graph is:

$$\mathbf{L} = \mathbf{l}_{i,j} = \begin{cases} 1 & \text{if } i = j \\ \frac{-1}{k} & \text{if } v_i \text{ and } v_j \text{ are adjacent} \\ 0 & \text{otherwise} \end{cases} \quad (1.4)$$

where k is the degree of each vertex v_1, \dots, v_n . So the following identity holds:

$$\mathbf{L} = I - \frac{1}{k} A$$

while for a general graph without isolated vertex we have:

$$\mathbf{L}_{i,j} = I - T^{-\frac{1}{2}} A T^{-\frac{1}{2}}$$

where A is the adjacency matrix of the graph G .

If $V(G) = \{v_1, \dots, v_n\}$ denote the set of the vertex of the graph G , let $C(G)$ be the vector space of all functions from $V(G)$ into \mathbb{R} . We have that $\dim C(G) = n$. Each element \mathbf{g} of $C(G)$ is usually written in the following form $\mathbf{g} = \sum_{i=1}^n g_i v^i$. In fact, if we think v^i as the function from $V(G)$ into \mathbb{R} such that

$$v^i(v_j) := \begin{cases} 1 & \text{if } i = j \\ 0 & \text{otherwise} \end{cases}$$

then $(v^1 \dots v^n)$ is a basis for $C(G)$ and the sum above expresses an element in term of the basis elements. Therefore, we can see the Laplacian like an operator $\mathbf{L} = C(G) \rightarrow C(G)$

$$\begin{aligned} \mathbf{L}g(v_j) &= g(v_j) + \sum_{v_j \sim v_i} \frac{-1}{\sqrt{d_{v_j} d_{v_i}}} g(v_i) = \\ &= \sum_{v_j \sim v_i} \frac{g(v_j)}{d_{v_j}} - \frac{g(v_i)}{\sqrt{d_{v_j} d_{v_i}}} \end{aligned}$$

that is equal to:

$$\mathbf{L}g(v_j) = \frac{-1}{d_{v_j}} \sum_{v_j \sim v_i} \left(\frac{g(v_j)}{\sqrt{d_{v_j}}} - \frac{g(v_i)}{\sqrt{d_{v_i}}} \right) \quad (1.5)$$

Since \mathbf{L} is symmetric with entries in \mathbb{R} its eigenvalues are real. Therefore we are allowed to use the variational characterization of the eigenvalues in terms of the Rayleigh quotient. Let g denote an arbitrary function that assigns to each vertex v_i a real value $g(v_i)$. Hence $g = (g(v_1), \dots, g(v_n))^T$ can be viewed like a column vector. Then:

$$\frac{\langle g, \mathbf{L}g \rangle}{\langle g, g \rangle} = \frac{\langle g, T^{-\frac{1}{2}} L T^{-\frac{1}{2}} g \rangle}{\langle g, g \rangle} =$$

If we put $f = T^{-\frac{1}{2}} g$ we have:

$$\frac{\langle f, Lf \rangle}{\langle T^{\frac{1}{2}} f, T^{\frac{1}{2}} f \rangle} = \frac{\sum_{v_i, v_j, i, j=1, \dots, n} l_{i,j} f(v_j) f(v_i)}{\sum_{v_i} f(v_i)^2 d_{v_i}} =$$

$$\begin{aligned} & \frac{\sum_{v_i} d_{v_i} f(v_i)^2 - \sum_{v_i \sim v_j} f(v_i) f(v_j) - \sum_{v_j \sim v_i} f(v_i) f(v_j)}{\sum_{v_i} f(v_i)^2 d_{v_i}} = \\ & \frac{\sum_{v_i \sim v_j} (f(v_i) - f(v_j))^2}{\sum_{v_i} f(v_i)^2 d_{v_i}} \end{aligned} \quad (1.6)$$

where $\sum_{v_i \sim v_j}$ denotes the sum over all the unordered pairs v_i, v_j for which v_i and v_j are adjacent. $\langle g, Lg \rangle, \langle g, g \rangle$ are standard inner products in \mathbb{R}^n . From equation 1.6 we can see that the eigenvalues of \mathbf{L} are all non negative.

Let $\mathbf{1}$ denote the function which value is 1 on each vertex, we have that $g = T^{\frac{1}{2}} \mathbf{1}$ is a eigenfunction with eigenvalue 0.

Let $0 = \lambda_0 \leq \lambda_1 \leq \lambda_2 \leq \dots \leq \lambda_{n-1}$ denote the eigenvalues of \mathbf{L} .

Definition 1.13. The set $\{\lambda_0, \dots, \lambda_{n-1}\}$ is said spectrum of the graph G .

As the eigenfunctions that refer to different eigenvalues are orthogonal, we have that

$$\lambda_G = \lambda_1 = \inf_{f \perp T\mathbf{1}} \frac{\sum_{v_i \sim v_j} (f(v_i) - f(v_j))^2}{\sum_{v_i} f(v_i)^2 d_{v_i}} \quad (1.7)$$

. with corresponding eigenfunction $g = T^{\frac{1}{2}} f$, while the non zero function f achieving 1.7 is said *harmonic eigenfunction* for L . We can express the largest eigenvalue in terms of the Rayleigh quotient:

$$\lambda_{n-1} = \sup_f \frac{\sum_{v_i \sim v_j} (f(v_i) - f(v_j))^2}{\sum_{v_i} f(v_i)^2 d_{v_i}} \quad (1.8)$$

. For a general k we have:

$$\begin{aligned} \lambda_k &= \inf_f \sup_{g \in P_{k-1}} \frac{\sum_{v_i \sim v_j} (f(v_i) - f(v_j))^2}{\sum_{v_i} f(v_i)^2 d_{v_i}} = \\ & \inf_{f \perp TP_{k-1}} \frac{\sum_{v_i \sim v_j} (f(v_i) - f(v_j))^2}{\sum_{v_i} f(v_i)^2 d_{v_i}} \end{aligned}$$

where P_{k-1} is the subspace generated by the harmonic eigenfunction corresponding to λ_i , for $i = 1, \dots, k-1$.

1.3 Eigenvalues upper and lower bounds for graphs

The main problems of spectral theory consist in deriving bounds on the distribution of eigenvalues and in analyzing the consequences and the impact of these bounds. In this section we state some upper and lower bounds; for example we will see that the eigenvalues of any graph lie between 0 and 2. The problem of delimiting the range of the eigenvalues for special classes of graphs represents an open-ended challenge in graphs theory.

Lemma 1.3.1. *For a graph G of n vertex, we have:*

1. $\sum_i \lambda_i \leq n$. *The equality holds if and only if G has not isolated vertices.*
2. *For $n \geq 2$,*

$$\lambda_1 \leq \frac{n}{n-1}$$

- . The equality holds if and only if G is the complete graph on n vertices.
For a graph G without isolated vertices we have:*

$$\lambda_{n-1} \geq \frac{n}{n-1}$$

3. $\lambda_1 \leq 1$, *if G is not a complete graph.*
4. $\lambda_1 > 0$, *if G is a connected graph. If $\lambda_i = 0$ and $\lambda_{i+1} \neq 0$, G has exactly $i + 1$ connected components.*
5. *For all $i \leq n - 1$, $\lambda_i \leq 2$, with $\lambda_{n-1} = 2$ if and only if a connected component of G is bipartite and non trivial.*
6. *The spectrum of a graph is the union of the spectra of its connected components.*

Proof. In order to prove item (i), we note that $trL \leq n$, and $trL = n$, if and only if the graph has not isolated vertices. As L is symmetric, the

spectral theorem affirms that we can decompose any symmetric matrix with the *symmetric eigenvalue decomposition*(SED) that is:

$$\mathbf{L} = \sum_{i=1}^n \lambda_i \phi_i \phi_i^T = U \Lambda U^T$$

$$\Lambda = \text{diag}(\lambda_0, \dots, \lambda_{n-1})$$

where the matrix of $U = [\phi_0, \dots, \phi_{n-1}]$ is orthogonal (that is $U^T U = U U^T = Id$) and the ϕ_i is the eigenfunction for the eigenvalue λ_i , $i = 0, \dots, n - 1$.

We have that:

$$\begin{aligned} \text{tr}(\mathbf{L}) &= \text{tr}(U \Lambda U^T) = \\ &= \text{tr}((U \Lambda) U^T) = \text{tr}(U^T U \Lambda) = \text{tr}(\Lambda) \end{aligned}$$

. Therefore we obtain that $\sum_i \lambda_i \leq n$, with equality holding if and only if G has not isolated vertices.

The inequalities in (ii) follow from (i) and $\lambda_0 = 0$.

In order to prove item (iii) suppose G contains two non adjacent vertices a , b and consider the function:

$$f(v_i) = \begin{cases} d_b & \text{if } v_i = a \\ -d_a & \text{if } v_i = b \\ 0 & \text{if } v_i \neq a, b \end{cases}$$

We have that f is orthogonal to $T\mathbf{1}$. In fact:

$$\langle f, T\mathbf{1} \rangle = \begin{pmatrix} 0 \\ \vdots \\ d_b \\ -d_a \\ 0 \\ \vdots \\ 0 \end{pmatrix} \cdot \begin{pmatrix} d_{v_1} \\ \vdots \\ d_a \\ d_b \\ \vdots \\ d_{v_i} \\ \vdots \\ d_{v_n} \end{pmatrix} =$$

$$\begin{aligned}
&= d_b d_a - d_a d_b = 0 \\
\lambda_1 &= \inf_{f \perp \mathbf{1}} \frac{\sum_{v_i, v_j \in E(G)} (f(v_i) - f(v_j))^2}{\sum_{v_i} f(v_i)^2 d_{v_i}} = \inf \frac{d_a d_b^2 + d_a^2 d_b}{d_a d_b^2 + d_a^2 d_b} = 1
\end{aligned}$$

Therefore, $\lambda_1 \leq 1$ follows for a not complete graph.

If G is connected the eigenvalue 0 has multiplicity 1 since, from 1.7, any harmonic eigenfunction with eigenvalue 0 assumes the same value at each vertex. Thus item (iv) follows from the fact that we can see a graph as the union of its connected components (each connected component is viewed as a distinct graph) and from the fact that the spectrum of the union of disjoint graphs is the union of the spectra of the original graphs. In order to show item (v), we use the fact that $(f(v_i) - f(v_j))^2 \leq 2(f(v_i)^2 + f(v_j)^2)$.

Moreover from the 1.8 we have that:

$$\begin{aligned}
\lambda_i &\leq \sup_f \frac{\sum_{v_i, v_j \in E(G)} (f(v_i) - f(v_j))^2}{\sum_{v_i} f(v_i)^2 d_{v_i}} \leq \\
&\leq \sup_f \frac{\sum_{v_i, v_j \in E(G)} 2(f(v_i)^2 + f(v_j)^2)}{\sum_{v_i} f(v_i)^2 d_{v_i}} \leq 2 \sup_f \frac{\sum_{v_i} f(v_i)^2 d_{v_i}}{\sum_{v_i} f(v_i)^2 d_{v_i}} \leq 2
\end{aligned}$$

for $i \leq n - 1$.

If we consider a function f such that $f(v_i) = -f(v_j)$ for every edge v_i, v_j , we have that:

$$\lambda_{n-1} = \sup_f \frac{\sum_{v_i \sim v_j} (f(v_i) - f(v_j))^2}{\sum_{v_i} f(v_i)^2 d_{v_i}} = 2 \frac{\sum_{v_i} f(v_i)^2 d_{v_i}}{\sum_{v_i} f(v_i)^2 d_{v_i}} = 2$$

. Therefore, since $f \neq 0$ G has a bipartite connected component. On the other hand, if G has a connected component which is bipartite, we can choose the function f as to make $\lambda_{n-1} = 2$. Item (vi) follows from definition. \square

Lemma 1.3.2. *The following statements are equivalent:*

1. G is bipartite
2. G has $i + 1$ connected components and $\lambda_{n-j} = 2$ for $1 \leq j \leq i$.
3. For each λ_i the value $2 - \lambda_i$ is also an eigenvalue of G .

Proof. (ii) \rightarrow (i) follows from items (iv) and (v) of the antecedent lemma considering a connected graph (a bipartite graph is in particular a connected graph). (iii) \rightarrow (ii) follows from item (iv) of the antecedent lemma considering a connected graph. In order to prove that (i) \rightarrow (iii), we consider a bipartite graph with vertex set consisting of two parts A and B . For any harmonic eigenfunction f with eigenvalue λ_k we consider the function g defined by

$$g(v_i) = \begin{cases} f(v_i) & \text{if } v_i \in A \\ -f(v_i) & \text{if } v_i \in B \end{cases}$$

We observe that for a general i , we have:

$$\lambda_i = \inf_{g \perp TP_{i-1}} \frac{\sum_{v_i \sim v_j} (g(v_i) - g(v_j))^2}{\sum_{v_i} g(v_i)^2 d_{v_i}}$$

where P_{i-1} is the subspace generated by the harmonic eigenfunctions corresponding to λ_i , for $i = 1, \dots, i-1$.

Therefore, by the expression of Rayleigh quotient we have :

$$\begin{aligned} & \frac{\sum_{v_i \sim v_j} (g(v_i) - g(v_j))^2}{\sum_{v_i} g(v_i)^2 d_{v_i}} = \\ & \frac{\sum_{v_i \sim v_j} (f(v_i) + f(v_j))^2}{\sum_{v_i} f(v_i)^2 d_{v_i}} = \\ & \frac{2 \sum_{v_i} f(v_i)^2 d_{v_i} + 2 \sum_{v_i \sim v_j} (f(v_i) f(v_j)) - \sum_{v_i} f(v_i)^2 d_{v_i}}{\sum_{v_i} f(v_i)^2 d_{v_i}} = \\ & \frac{2 \sum_{v_i} f(v_i)^2 d_{v_i} + 2 \sum_{v_i \sim v_j} (f(v_i) f(v_j)) - \sum_{v_i} f(v_i)^2 d_{v_i}}{\sum_{v_i} f(v_i)^2 d_{v_i}} = \\ & \frac{2 \sum_{v_i} f(v_i)^2 d_{v_i} + \sum_{v_i \sim v_j} (f(v_i) - f(v_j))^2}{\sum_{v_i} f(v_i)^2 d_{v_i}} = \\ & 2 - \frac{\sum_{v_i \sim v_j} (f(v_i) - f(v_j))^2}{\sum_{v_i} f(v_i)^2 d_{v_i}} = 2 - \lambda_k \end{aligned}$$

as f is an harmonic eigenfunction of \mathbf{L} achieving λ_k .

The statement follows by considering:

$$\inf_{g \perp TP_{i-1}} \frac{\sum_{v_i \sim v_j} (g(v_i) - g(v_j))^2}{\sum_{v_i} g(v_i)^2 d_{v_i}} = 2 - \lambda_k$$

□

In order to improve the lower bound for λ_1 , we will introduce two important definitions:

Definition 1.14. For any pair of vertices v_i, v_j the number of edges in the shortest path joining v_i and v_j is said *distance* between v_i and v_j and is denoted by $d(v_i, v_j)$.

Definition 1.15. The *diameter* of a graph is the maximum distance over all pairs of vertices of G .

Lemma 1.3.3. Let G denote a connected graph with diameter D . Therefore we have that:

$$\lambda_1 \geq \frac{1}{D \text{vol}G}$$

where $\text{vol}(G) = \sum_{v_i} d_{v_i}$.

Proof. Suppose f a harmonic eigenfunction archieving λ_1 as in 1.7. Let v_0^* denote a vertex such that $|f(v_0^*)| = \max_{v_i} |f(v_i)|$. Since $\sum f(v_i) d_{v_i} = 0$ there exists a vertex v_1^* such that $f(v_1^*) f(v_0^*) < 0$. We call P the shortest path that joins v_0^* and v_1^* . Then we have:

$$\begin{aligned} \lambda_1 &= \inf_{f \perp T1} \frac{\sum_{v_i, v_j \in E(G)} (f(v_i) - f(v_j))^2}{\sum_{v_i} f(v_i)^2 d_{v_i}} \geq \\ &\geq \frac{\sum_{v_i, v_j \in P} (f(v_i) - f(v_j))^2}{\text{vol}G f(v_0^*)^2} \geq \frac{\frac{1}{D} (f(v_0^*) - f(v_1^*))^2}{\text{vol}G f(v_0^*)^2} \geq \frac{1}{D \text{vol}G} \end{aligned}$$

by using Cauchy-Schwartz inequality.

□

Lemma 1.3.4. *For any vertex $v_i \in V(G)$ the following equality holds:*

$$\frac{1}{v_i} \sum_{v_j \sim v_i} (f(v_i) - f(v_j)) = \lambda_G f(v_i)$$

where f is an harmonic eigenfunction archieving λ_G in 1.7.

Proof. For a fixed $v_0 \in V(G)$ let f define the following function:

$$f_\varepsilon(v_j) = \begin{cases} f(v_0) + \frac{\varepsilon}{d_{v_0}} & \text{if } v_j = v_0 \\ f(v_j) - \frac{\varepsilon}{\text{vol}G - d_{v_0}} & \text{otherwise} \end{cases}$$

. We have that:

$$\begin{aligned} & \frac{\sum_{v_i, v_j \in E(G)} (f_\varepsilon(v_i) - f_\varepsilon(v_j))^2}{\sum_{v_i} f_\varepsilon(v_i)^2 d_{v_i}} = \\ & = \frac{\sum_{v_i, v_j \in E(G)} (f(v_i) - f(v_j))^2 + \sum_{v_j \sim v_0} \frac{2\varepsilon(f(v_0) - f(v_j))}{d_{v_0}} - \sum_{v_j \neq v_0} \sum_{v_j \sim v'_j} \frac{2\varepsilon(f(v_j) - f(v'_j))}{\text{vol}G - d_{v_0}}}{\sum_{v_i \in V(G)} f^2(v_i) d_{v_i} + 2\varepsilon f(v_0) - \frac{2\varepsilon}{\text{vol}G - d_{v_0}} \sum_{v_j \neq v_0} f(v_j) d_{v_j}} + O(\varepsilon^2) = \\ & \frac{\sum_{v_i, v_j \in E(G)} (f(v_i) - f(v_j))^2 + \sum_{v_j \sim v_0} \frac{2\varepsilon(f(v_0) - f(v_j))}{d_{v_0}} + \sum_{v_j \sim v_0} \frac{2\varepsilon(f(v_0) - f(v_j))}{\text{vol}G - d_{v_0}}}{\sum_{v_i \in V(G)} f^2(v_i) d_{v_i} + 2\varepsilon f(v_0) - \frac{2\varepsilon f(v_0) d_{v_0}}{\text{vol}G - d_{v_0}}} + O(\varepsilon^2) = \end{aligned}$$

since $\sum_{v_i \in V(G)} f(v_i) d_{v_i} = 0$ and $\sum_{v_j} \sum_{v'_j} (f(v_j) - f(v'_j)) = 0$. From definition 1.7, we have that:

$$\frac{\sum_{v_i, v_j \in E(G)} (f_\varepsilon(v_i) - f_\varepsilon(v_j))^2}{\sum_{v_i} f_\varepsilon(v_i)^2 d_{v_i}} \geq \frac{\sum_{v_i, v_j \in E(G)} (f(v_i) - f(v_j))^2}{\sum_{v_i} f(v_i)^2 d_{v_i}} =$$

. If we consider:

$$\begin{aligned} & \lim_{\varepsilon \rightarrow 0} \frac{\sum_{v_i, v_j \in E(G)} (f_\varepsilon(v_i) - f_\varepsilon(v_j))^2}{\sum_{v_i} f_\varepsilon(v_i)^2 d_{v_i}} = \\ & \frac{\sum_{v_i, v_j \in E(G)} (f(v_i) - f(v_j))^2}{\sum_{v_i} f(v_i)^2 d_{v_i}} = \lambda_G \end{aligned}$$

as f is an harmonic eigenfunction archieving λ_G .

Therefore we have that:

$$\sum_{v_i, v_j \in E(G)} (f(v_i) - f(v_j))^2 + 2\varepsilon \left(\sum_{v_j: v_j \sim v_0} f(v_0) - f(v_j) \right) \left(\frac{\text{vol}G}{d_{v_0}(\text{vol}G - d_{v_0})} \right) =$$

$$\lambda_G \left(\sum_{v_i} f^2(v_i) d_{v_i} \right) + \lambda_G \left(\frac{2\varepsilon \text{vol}G f(v_0)}{\text{vol}G - d_{v_0}} \right) =$$

$$\frac{\text{vol}G}{d_{v_0}(\text{vol}G - d_{v_0})} \sum_{v_j \sim v_0} f(v_0) - f(v_j) = \lambda_G \frac{\text{vol}G f(v_0)}{\text{vol}G - d_{v_0}}$$

. Finally, we can conclude that:

$$\frac{\sum_{v_j \sim v_0} f(v_0) - f(v_j)}{d_{v_0}} = \lambda_G f(v_0)$$

□

1.4 The Laplacian of a weighted graph

Definition 1.16. Given a set of vertices $V(G) = \{v_1, \dots, v_n\}$, a weighted graph $G = \{V(G), E(G)\}$ (possibly with loops) is a graph with an associated weight function:

$$w : V(G) \times V(G) \longrightarrow \mathbb{R}$$

such that:

$$w(v_i, v_j) = w(v_j, v_i)$$

and

$$w(v_i, v_j) \geq 0$$

$\forall i, j = 1, \dots, n$

Remark 2. If $\{v_i, v_j\}$ are not in $E(G)$, $w(v_i, v_j) = 0$.

Remark 3. Unweighted graphs are a particular case of weighted graphs in which all the weights are 0 or 1. Therefore all the definitions and subsequent theorems for simple graphs can be easily extended to weighted graphs.

Definition 1.17. In a weighted graph the degree of a vertex v_i is given by:

$$d_{v_i} = \sum_{v_j=1}^n w(v_i, v_j)$$

and $\text{Vol}G = \sum_i d_{v_i}$

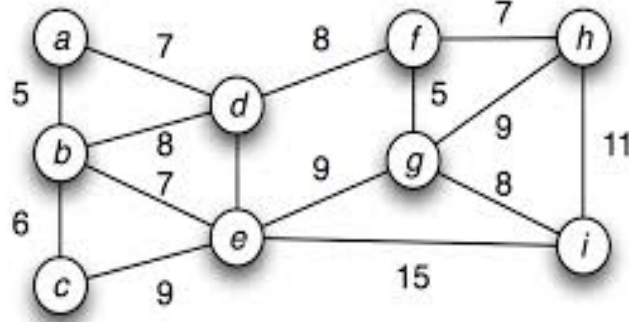


Figure 1.4: Example of weighted graph

Let L be the following $n \times n$ matrix:

$$L_{i,j} = \begin{cases} \sum_{i,j': e_{i,j'} \in E(G)} w(v_i, v_{j'}) & \text{if } i = j \\ -w(v_i, v_j) & \text{if } v_i \text{ and } v_j \text{ are adjacent} \\ 0 & \text{otherwise} \end{cases} \quad (1.9)$$

For a function $f : V(G) \rightarrow \mathbb{R}$ we have:

$$Lf(x) = \sum_{v_j: v_i \sim v_j} (f(v_i) - f(v_j))w(v_i, v_j)$$

The Laplacian of a weighted graph is defined to be

$$\mathbf{L} = T^{-\frac{1}{2}} L T^{-\frac{1}{2}}$$

where T is the diagonal matrix with the (i, i) th entry having the value d_{v_i} .

Therefore \mathbf{L} is the following $n \times n$ matrix:

$$\mathbf{L}_{i,j} = \begin{cases} 1 - \frac{w(v_i, v_i)}{d_{v_i}} & \text{if } i = j \\ \frac{-w(v_i, v_j)}{\sqrt{d_{v_i} d_{v_j}}} & \text{if } v_i \text{ and } v_j \text{ are adjacent} \\ 0 & \text{otherwise} \end{cases} \quad (1.10)$$

We can use the same characterization for the eigenvalues of the generalized version of \mathbf{L} . In fact we have:

$$\begin{aligned} \lambda_G = \lambda_1 &= \inf_{g \perp T^{\frac{1}{2}} \mathbf{1}} \frac{\langle g, \mathbf{L}g \rangle}{\langle g, g \rangle} = \\ &= \inf_{f: \sum f(v_i) d_{v_i} = 0} \frac{\sum_{v_i \in V(G)} (f(v_i) Lf(v_i))}{\sum_{v_i} f(v_i)^2 d_{v_i}} = \\ &= \inf_{f: \sum f(v_i) d_{v_i} = 0} \frac{\sum_{v_i \sim v_j} (f(v_i) - f(v_j))^2 w(v_i, v_j)}{\sum_{v_i} f(v_i)^2 d_{v_i}} \end{aligned} \quad (1.11)$$

and

$$\lambda_{n-1} = \sup_f \frac{\sum_{v_i \sim v_j} (f(v_i) - f(v_j))^2 w(v_i, v_j)}{\sum_{v_i} f(v_i)^2 d_{v_i}} \quad (1.12)$$

. For a general k the eigenvalues are given by:

$$\begin{aligned} \lambda_k &= \inf_f \sup_{g \in P_{k-1}} \frac{\sum_{v_i \sim v_j} (f(v_i) - f(v_j))^2 w(v_i, v_j)}{\sum_{v_i} f(v_i)^2 d_{v_i}} = \\ &= \inf_{f \perp TP_{k-1}} \frac{\sum_{v_i \sim v_j} (f(v_i) - f(v_j))^2 w(v_i, v_j)}{\sum_{v_i} f(v_i)^2 d_{v_i}} \end{aligned} \quad (1.13)$$

where P_{k-1} is the subspace generated by the harmonic eigenfunctions corresponding to λ_i , for $i = 1, \dots, k-1$.

Chapter 2

From graphs to manifolds: relationship between discrete and continuous case

There are many similarities between the Laplace operator on compact Riemannian manifold that is generated by Riemannian metric and the Laplacian for finite graphs, that comes from the adjacency relation. Moreover it is important to underline that the discrete and the continuous cases sometimes can be analyzed by an universal approach. In this chapter we will derive first some eigenvalues-diameter inequalities for graphs and then we will apply these discrete methods in order to derive new eigenvalues upper bounds for compact Riemannian manifolds.

2.1 Eigenvalues and diameter of a graph

The diameter is an important combinatorial invariant for a graph that has a wide range of applications as for example in communication network's models or in performance analysis and cost optimization. There is a strict relationship between the diameter of the graph and the eigenvalues based on the following observation: let M denote a $n \times n$ matrix in which the

rows and the columns are indexed by the vertices of G . Moreover M has the propriety that $M(v_i, v_j) = 0$ if v_i, v_j are not adjacent. Suppose that we can show that for some integer t and some polynomial $p_t(x)$ of degree t we have $p_t(M)(v_i, v_j) \neq 0 \forall v_i, v_j$. It means that the maximum distance over all pairs of vertices is at most t i.e $D(G) \leq t$. This allows us to derive some diameter-eigenvalue inequalities starting from distance between two subsets inequalities.

Theorem 2.1.1. *In a graph G let X, Y be two subsets of $V(G)$ such that $d(X, Y) \geq 2$ and let \bar{X}, \bar{Y} be the complements of respectively X, Y in $V(G)$. We have:*

$$d(X, Y) = \lceil \frac{\ln(\sqrt{\text{vol}\bar{X}\text{vol}\bar{Y}\text{vol}X\text{vol}Y})}{\ln(\frac{\lambda_{n-1}+\lambda_1}{\lambda_{n-1}-\lambda_1})} \rceil \quad (2.1)$$

Proof. For $X \subseteq V(G) = v_1, \dots, v_n$, we consider the characteristic function ψ_X :

$$\psi_X(v_i) = \begin{cases} 1 & \text{if } v_i \in X \\ 0 & \text{otherwise} \end{cases}$$

with $i = 1, \dots, n$. In the same way we define ψ_Y . The previous remark suggests that if we can show that for some integer t and some polynomial $p_t(z)$ of degree t

$$\langle T^{\frac{1}{2}}\psi_Y, p_t(\mathbf{L})(T^{\frac{1}{2}}\psi_X) \rangle > 0$$

then there is a path of length at most t joining a vertex in X to a vertex in Y .

Therefore, by definition, we have $d(X, Y) \leq t$.

We consider the fourier series of the function $T^{\frac{1}{2}}\psi_X$ i.e.:

$$T^{\frac{1}{2}}\psi_X = \sum_{i=0}^{n-1} a_i \phi_i$$

where a_i are the Fourier coefficients and ϕ_i are orthogonal eigenfunctions of G . As $\phi_0 = T^{\frac{1}{2}}\mathbf{1}$ is the eigenfunction associated to the eigenvalue λ_0 , we

have:

$$a_0 = \frac{\langle T^{\frac{1}{2}}\psi_X, T^{\frac{1}{2}}\mathbf{1} \rangle}{\|T^{\frac{1}{2}}\mathbf{1}\|} = \frac{\left(\begin{array}{c} \left(\begin{array}{c} \sqrt{d_{v_i}} \text{ if } v_i \in X \\ 0 \text{ otherwise} \end{array} \right) \cdot \left(\sqrt{d_{v_1}} \ \dots \ \sqrt{d_{v_n}} \right) \end{array} \right)}{\| \sqrt{d_{v_1}} \ \dots \ \sqrt{d_{v_n}} \|} = \frac{\text{vol}X}{\sqrt{\text{vol}G}}$$

. Let b_i define the Fourier coefficients of ψ_Y i.e.:

$$T^{\frac{1}{2}}\psi_Y = \sum_{i=0}^{n-1} b_i \phi_i$$

We choose $p_t(z) = \left(1 - \frac{2z}{\lambda_1 + \lambda_{n-1}}\right)^t$. As G is not a complete graph for the Lemma 1.3.1 $\lambda_1 \neq \lambda_{n-1}$ and

$$|p_t(\lambda)| \leq (1 - \lambda)^t$$

for all $i = 0, \dots, n-1$ where $\lambda = \frac{2\lambda_1}{\lambda_1 + \lambda_{n-1}}$. We have:

$$\begin{aligned} \langle T^{\frac{1}{2}}\psi_Y, p_t(\mathbf{L})(T^{\frac{1}{2}}\psi_X) \rangle &= \left\langle \sum_i b_i \phi_i, \left(\sum_i p(\lambda_i) \phi_i \phi_i^T \right) \left(\sum_i a_i \phi_i \right) \right\rangle = \\ & a_0 b_0 + \sum_{i>0} p_t(\lambda_i) a_i b_i \geq a_0 b_0 - (1 - \lambda)^t \sqrt{\sum_{i>0} a_i^2 \sum_{i>0} b_i^2} \end{aligned} \quad (2.2)$$

by using Cauchy-Schwarz inequality. If we consider:

$$\sum_{i>0} a_i^2 = \|T^{\frac{1}{2}}\psi_X\|^2 - a_0^2 = \text{vol}X - \frac{\text{vol}X^2}{\text{vol}G} = \frac{\text{vol}X \text{vol}\bar{X}}{\text{vol}G}$$

Therefore the equation in 2.2 becomes:

$$\langle T^{\frac{1}{2}}\psi_Y, p_t(\mathbf{L})(T^{\frac{1}{2}}\psi_X) \rangle \geq \frac{\text{vol}X \text{vol}Y}{\text{vol}G} - (1 - \lambda)^t \frac{\sqrt{\text{vol}X \text{vol}\bar{X} \text{vol}Y \text{vol}\bar{Y}}}{\text{vol}G}$$

If the inequality in 2.2 is strict,

$$\langle T^{\frac{1}{2}}\psi_Y, p_t(\mathbf{L})(T^{\frac{1}{2}}\psi_X) \rangle > 0 \iff \frac{\text{vol}X \text{vol}Y}{\text{vol}G} - (1 - \lambda)^t \frac{\sqrt{\text{vol}X \text{vol}\bar{X} \text{vol}Y \text{vol}\bar{Y}}}{\text{vol}G} \geq 0$$

Therefore, we have:

$$-(1 - \lambda)^t \frac{\sqrt{\text{vol}X \text{vol}\bar{X} \text{vol}Y \text{vol}\bar{Y}}}{\text{vol}G} \geq -\frac{\text{vol}X \text{vol}Y}{\text{vol}G}$$

$$\begin{aligned} \frac{1}{(1-\lambda)^t} &\geq \frac{\sqrt{\text{vol}\bar{X}\text{vol}\bar{Y}}}{\sqrt{\text{vol}X\text{vol}Y}} \\ t &\geq \frac{\ln\left(\frac{\sqrt{\text{vol}\bar{X}\text{vol}\bar{Y}}}{\sqrt{\text{vol}X\text{vol}Y}}\right)}{\ln\left(\frac{1}{(1-\lambda)^t}\right)} \end{aligned} \quad (2.3)$$

Then, if we choose a t as in 2.3 we have

$$\langle T^{\frac{1}{2}}\psi_Y, p_t(\mathbf{L})(T^{\frac{1}{2}}\psi_X) \rangle > 0$$

and $d(X, Y) \leq t$. If in 2.2 the equality holds, we have that $|b_i| = |ca_i|$ for some c and $i > 0$. Moreover the equality

$$a_i b_i p_i(\lambda_i) = -|a_i b_i| |p_i(\lambda_i)| = -|a_i b_i| (1-\lambda)^t$$

implies that there exists an integer k , $1 \leq k < n-1$ such that $b_i = -ca_i$, $\lambda_i = \lambda_1$ for $i = 1, \dots, k$ and for $i > k$, $b_i = ca_i$ and $\lambda_i = \lambda_{n-1}$. Since

$$\langle T^{\frac{1}{2}}\psi_Y, \mathbf{L}(T^{\frac{1}{2}}\psi_X) \rangle = \sum_{i>0} a_i b_i \lambda_i = 0$$

we have:

$$-\lambda_1 \sum_{i=1}^k a_i^2 + \lambda_{n-1} \sum_{i>k} a_i^2 = 0$$

and $\sum_{i=1}^k a_i^2 = \frac{\lambda_{n-1} \sum_{i>k} a_i^2}{\lambda_1}$. We consider for $t \geq 2$

$$\langle T^{\frac{1}{2}}\psi_Y, \mathbf{L}(T^{\frac{1}{2}}\psi_X) \rangle \geq c \left(-\lambda_1^t \sum_{i=1}^k a_i^2 + \lambda_{n-1}^t \sum_{i>k} a_i^2 \right) \geq c(-\lambda_1^{t-1} \lambda_{n-1} + \lambda_{n-1}^t) \sum_{i>k} a_i^2 > 0$$

Therefore $d(X, Y) \leq t$. □

An immediate consequence is the following corollary

Corollary 2.1.2. *For a regular graph which is not complete we have:*

$$D(G) \leq \frac{\ln(n-1)}{\ln\left(\frac{\lambda_{n-1} + \lambda_1}{\lambda_{n-1} - \lambda_1}\right)}$$

2.2 Eigenvalues upper bounds for manifolds

Let (M, g) denote a connected, compact Riemannian manifold. We will consider the Laplace-Beltrami operator, that is a linear, differential operator of the second order:

$$\Delta : C^\infty(M) \rightarrow C^\infty(M) \Delta f := -\operatorname{div}(\operatorname{grad}(f))$$

. The eigenvalues problems have the following formulation:

- Closed problem:

$$\Delta f = \lambda f \in M; \partial M = \emptyset \quad (2.4)$$

- Dirichlet problem:

$$\Delta f = \lambda f \in M_{\setminus \partial M}, f = 0 \text{ in } \partial M; \partial M \neq \emptyset \quad (2.5)$$

- Neumann problem:

$$\Delta f = \lambda f \in M_{\setminus \partial M}; \left(\frac{df}{d\eta}\right)_{|\partial M} = 0; \partial M \neq \emptyset \quad (2.6)$$

where $\frac{df}{d\eta}$ is the derivative of f in the direction of the outward unit normal vector field η on ∂M .

Definition 2.1. $L^2(M)$ denotes the space of the measurable functions on M such that

$$\int_M |f|^2 dv_g(x) < \infty$$

where v_g is the canonic measure on M

Remark 4. $L^2(M)$ is the completion of $C^\infty(M)$ with respect to the inner product:

$$(f_1, f_2)_g = \int_M f_1(x) f_2(x) dv_g(x)$$

and $\|f\|_L^2(M) = (f, f)_g^{\frac{1}{2}}$ is the induced norm.

A classical result holds:

Theorem 2.2.1. *Let M be a compact manifold with boundary ∂M (eventually empty) and consider the above mentioned eigenvalue problems. Then:*

1. *The set of the eigenvalues consists of an infinite sequence $0 < \lambda_1 \leq \lambda_2 \leq \dots \rightarrow \infty$ where 0 is not an eigenvalue in the Dirichlet problem.*
2. *Each eigenvalue has finite multiplicity and the eigenspaces corresponding to distinct eigenvalues are $L^2(M)$ -orthogonal.*
3. *The direct sum of the eigenspaces $E(\lambda_i)$ is dense in $L^2(M)$ for the L^2 -norm. Furthermore, each eigenfunction is C^∞ smooth and analytic.*

In order to investigate the Laplace-Bertami equation $\Delta f = \lambda f$, it's very relevant to look at the variational characterization of the spectrum.

Let us introduce the Rayleigh quotient:

$$R(f) = \frac{\|df\|_{L^2(M)}^2}{\|f\|_{L^2(M)}^2} = \frac{(df, df)}{(f, f)} \quad (2.7)$$

where f lies in the Sobolev space $H^1(M)$ in the closed and Neumann problems and in H_0^1 in the Dirichlet problem.

In fact we have:

$$R(f) = \frac{(\Delta f, f)}{(f, f)} = \frac{\int_M \langle df, df \rangle dv_g - \int_{\partial M} f \frac{\partial f}{\partial \eta} da_g}{\int_M |f|^2 dv_g} = \frac{\int_M |df|^2 dv_g}{\int_M |f|^2 dv_g} = \frac{(df, df)}{(f, f)}$$

by using Green formula. We observe that da_g is the volume form on ∂M and the integral $\int_{\partial M} f \frac{\partial f}{\partial \eta} da_g = 0$ in any of the three eigenvalue problems (closed problem, Dirichlet and Neumann boundary conditions). In the case where f is an eigenfunction with eigenvalue λ_k we have:

$$R(f) = \lambda_k$$

. The variational characterization of the spectrum is expressed by the following theorem:

Theorem 2.2.2. *Let us consider one of the three eigenvalue problems. Let f_i denote an orthonormal system of eigenfunctions associated to the eigenvalues λ_i .*

1. We have:

$$\lambda_k = \inf\{R(f) : f \neq 0; f \perp f_0, \dots, f_{k-1}\}$$

where $f \in H^1(M)$ (or $H_0^1(M)$) in the Dirichlet problem and $R(f) = \lambda_k$ if and only if f is an eigenfunction for λ_k .

In particular for a compact Riemannian manifold without boundary, we have:

$$\lambda_1 = \inf\{R(f) \text{ such that } f \neq 0; \int_M f dv_g = 0\}$$

2. Min-Max: we have

$$\lambda_k = \inf_{V_k} \sup\{R(f) : f \neq 0; f \in V_k\}$$

where V_k runs through $k + 1$ dimensional subspaces of $H^1(M)$ (K dimensional subspaces of $H_0^1(M)$ for the Dirichlet problem).

In particular, the following inequality holds:

$$\lambda_k(M, g) \leq \sup R(f) : f \neq 0; f \in V$$

for any given $k + 1$ -dimensional vector subspace V of $H^1(M)$.

Moreover, if V_k is generated by $k + 1$ disjointly supported functions f_1, \dots, f_{k+1} we have:

$$\sup\{R(f) : f \neq 0; f \in V_k\} = \sup\{R(f_i), i = 1, \dots, k + 1\}$$

Remark 5. We can observe that there is a natural correspondence between equation 1.7 and the expression of the eigenvalue of the Laplace-Bertrami operator for compact Riemannian manifold without boundary $\lambda_M = \inf \frac{\int_M (|f|)^2 dv_g}{\int_M f^2 dv_g}$ where f ranges over the functions satisfying $\int_M f dv_g = 0$

A parallelism between discrete and continuous case can be established. In order to show how discrete methods used in the previous section for deriving eigenvalues-diameter inequalities can be applied to derive new eigenvalues upper bounds for compact Riemannian manifolds, we will refer to a general setting that consists clearly in a underlying space with a finite measure, in

a well-defined Laplace operator \mathbf{L} on functions on M such that \mathbf{L} is a self-adjoint operator with discrete spectrum, in boundary conditions that do not disrupt the self-adjointness of \mathbf{L} , in an appropriate distance function on M .

Remark 6. The boundary conditions described in 2.4, 2.5, 2.6 satisfy these assumptions.

In order to derive eigenvalues upper bounds for compact Riemannian manifolds we will expose first some facts about graphs that will be treated according to this general setting.

Remark 7. For a finite connected graph G the metric, that we denote by μ , is given by the degree of each vertex.

Definition 2.2. If $f \in L^2(G, \mu)$, $r \in \mathbb{R}$ we have:

$$\text{supp}_r f = \{x \in G \text{ such that } d(x, f) \leq r\}$$

where $d(x, y)$ is the distance function.

Let p_s denote a polynomial of degree s , then we have

$$\text{supp}_{p_s}(\mathbf{L})f \subset \text{supp}_s f \tag{2.8}$$

An analogous version of 2.8 can be given for a Riemannian compact manifold.

Definition 2.3. If $f \in L^2(M, v_g)$, $r \in \mathbb{R}$ we have:

$$\text{supp}_r f = \{x \in M \text{ such that } \text{dist}(x, \text{supp} f) \leq r\}$$

where $\text{dist}(x, y)$ is a distance function on $M \times M$ which is Lipschitz and satisfies $|\nabla \text{dist}(x, y)| \leq 1$.

There exists a non trivial family of bounded continuous functions $P_s(\lambda)$ defined on the spectrum $\text{spec} \mathbf{L}$, where $s \in [0, \infty)$, such that for any $f \in L^2(M, v_g)$ we have:

$$\text{supp} P_s(\mathbf{L})f \subset \text{supp}_s f$$

Definition 2.4. We consider:

$$p(s) = \sup_{\lambda \in \text{spec} \mathbf{L}} |P_s(\lambda)|$$

where we assume that $p(s)$ is locally integrable.

Definition 2.5. Let us define

$$\Phi(\lambda) = \int_0^\infty \phi(s) P_s(\lambda) ds$$

where $\phi(s)$ is a measurable function on $(0, \infty)$ such that

$$\int_0^\infty |\phi(s)| p(s) ds < \infty$$

In particular, $\Phi(\lambda)$ is a bounded function on $\text{spec} \mathbf{L}$, and we can apply the operator $\Phi(\mathbf{L})$ to any function in $L^2(M, v_g)$.

Lemma 2.2.3. *The following inequality holds:*

$$\|\Phi(\mathbf{L})\|_{L^2(M \setminus \text{supp}_r f)} \leq \|f\|_2 \int_r^\infty |\Phi(s)| p(s) ds$$

where $f \in L^2(M, v_g)$ and $\|f\|_2 = \|f\|_{L^2(M, v_g)}$

Proof. We denote by

$$w(x) = \Phi(\mathbf{L})f(x) = \int_0^\infty \Phi(s) P_s(\mathbf{L})f(x) ds$$

Let us consider a point x that is not in the $\text{supp}_r f$. As $\text{supp} P_s(\mathbf{L}) \subset \text{supp}_s f$, we have that $P_s(\mathbf{L})f(x) = 0$ whenever $s \leq r$. Therefore, for those points

$$w(x) = \int_r^\infty \Phi(s) P_s(\mathbf{L})f(x) ds$$

and

$$\begin{aligned} \|w\|_{L^2(M \setminus \text{supp}_r f)} &\leq \left\| \int_r^\infty \phi(s) P_s(\mathbf{L})f(x) ds \right\|_2 \leq \\ &\leq \int_r^\infty \left(\int_M (\phi(s) P_s(\mathbf{L})f(x))^2 dv_g \right)^{\frac{1}{2}} ds \leq \\ &\leq \|f\|_2 \int_r^\infty |\phi(s)| p(s) ds \end{aligned}$$

□

Corollary 2.2.4. *If $f, g \in L^2(M, v_g)$ and let D denote the distance between $\text{supp}f$ and $\text{supp}g$, then:*

$$\left| \int_M f \Phi(\mathbf{L}) g dv_g \right| \leq \|f\|_2 \|g\|_2 \int_D^\infty |\phi(s)| p(s) ds \quad (2.9)$$

Proof. We consider :

$$\int_M f \Phi(\mathbf{L}) g dv_g = \int_M \left(\int_0^\infty \phi(s) P_s(\mathbf{L}) f(x) ds \right) g dv_g \quad (2.10)$$

Then, by definition 2.10 is zero out of the $\text{supp}g$. Therefore 2.9 becomes

$$\int_{\text{supp}g} \left(\int_0^\infty \phi(s) P_s(\mathbf{L}) f(x) ds \right) g dv_g$$

. If the point x is not in the $\text{supp}_D f$, $P_s(\mathbf{L}) f(x) = 0$ whenever $s \leq D$, because $\text{supp}P_s(\mathbf{L}) \subset \text{supp}_s f$. Then, we have :

$$\begin{aligned} & \left| \int_{\text{supp}g} \left(\int_0^\infty \phi(s) P_s(L) f(x) ds \right) g dv_g \right| \leq \\ & \left| \int_{M \setminus \text{supp}_D f} \left(\int_D^\infty \phi(s) P_s(\mathbf{L}) f(x) ds \right) g dv_g \right| \leq \\ & \leq \|f\|_2 \|g\|_2 \int_D^\infty |\phi(s)| p(s) ds \end{aligned}$$

by Holder inequality. □

If we choose $P_s(\lambda) = \cos(\sqrt{\lambda}s)$ and $\phi(s) = \frac{1}{\sqrt{\pi t}} e^{-\frac{s^2}{4t}}$, we have:

$$\Phi(\lambda) = \int_0^\infty \Phi(s) P_s(\lambda) f(x) ds = e^{-\lambda t}$$

By using the previous corollary we have proved

Corollary 2.2.5. *If $f, g \in L^2(M, v_g)$ and let D denote the distance between $\text{supp}f$ and $\text{supp}g$, then:*

$$\left| \int_M f e^{-\mathbf{L}t} g dv_g \right| \leq \|f\|_2 \|g\|_2 \int_D^\infty \frac{1}{\sqrt{\pi t}} e^{-\frac{s^2}{4t}} ds \quad (2.11)$$

A similar but weaker result that will be useful is the following corollary:

Corollary 2.2.6.

$$\left| \int_M f e^{-Lt} g dv_g \right| \leq \|f\|_2 \|g\|_2 e^{-\frac{D^2}{4t}} \quad (2.12)$$

The main result of this chapter is the following theorem:

Theorem 2.2.7. *For two arbitrary disjoint sets X, Y on M we have:*

$$\lambda_1 = \frac{1}{\text{dist}(X, Y)^2} \left(1 + \log \frac{(v_g(M))^2}{v_g(X)v_g(Y)} \right)^2 \quad (2.13)$$

Moreover, if X_0, \dots, X_k are $k+1$ disjoint subsets such that $\text{dist}(X_i, Y_j) \geq D$, $\forall i, j = 0, \dots, k$ and $D > 0$, we have for any $k \geq 1$

$$\lambda_1 = \frac{1}{D^2} \left(1 + \sup_{i \neq j} \ln \frac{(v_g(M))^2}{v_g(X_i)v_g(X_j)} \right)^2 \quad (2.14)$$

Proof. Let $\{\phi_i\}$ be an orthonormal frame of eigenfunctions in $L^2(M)$. In order to prove the theorem, we consider the heat equation with Robin boundary conditions:

$$\begin{aligned} \frac{\partial}{\partial t} u(x, t) - \Delta u(x, t) &= 0 \quad (x, t) \in M \times \mathbb{R}^+ \\ \alpha(x)u(x, t) + \beta(x) \frac{\partial u(x, t)}{\partial \eta} &= 0 \quad (x, t) \in \partial M \times \mathbb{R}^+ \end{aligned}$$

where $\alpha(x)$ and $\beta(x)$ are non negative smooth functions on ∂M such that $\alpha(x) + \beta(x) > 0 \forall x \in \partial M$. The heat equation admits unique fundamental solution that we denote by $p(x, y, t)$. If we consider the eigenvalue expansion, we have that:

$$p(x, y, t) = \sum_{i=0}^{+\infty} e^{-\lambda_i t} \phi_i(x) \phi_i(y)$$

By using the previous corollary we have the following estimate:

$$\int_X \int_Y p(x, y, t) f(x) g(y) dv_g(x) dv_g(y) \leq \left(\int_X f^2 \int_Y g^2 \right)^{\frac{1}{2}} e^{-\frac{D^2}{4t}}$$

for any functions $f, g \in L^2(M)$ and for any two disjoint Borel set $X, Y \subset M$, where $D = \text{dist}(X, Y)$. We start with the case $k = 2$. We integrate the eigenvalue expansion:

$$I(f, g) = \int_X \int_Y p(x, y, t) f(x) g(y) dv_g(x) dv_g(y) = \sum_{i=0}^{\infty} e^{-\lambda_i t} \int_X f \phi_i \int_Y g \phi_i$$

Let f_i denote the Fourier coefficients of the function $f\psi_X$ and g_i denote those of the function $g\psi_Y$ with respect to the frame ϕ_i , where ψ_X is a characteristic function:

$$\psi_X(x) = \begin{cases} 1 & \text{if } x \in X \\ 0 & \text{otherwise} \end{cases}$$

We have:

$$I(f, g) = e^{-\lambda_0 t} f_0 g_0 + \sum_{i=0}^{\infty} e^{-\lambda_i t} f_i g_i \quad (2.15)$$

The following inequalities hold:

$$|e^{-\lambda_i t} f_i g_i| \leq e^{-\lambda_1 t} \left(\sum_{i=0}^{\infty} f_i^2 \sum_{i=0}^{\infty} g_i^2 \right)^{\frac{1}{2}} \leq e^{-\lambda_1 t} \|f\psi_X\|_2 \|g\psi_Y\|_2$$

where we use Parseval theorem. Therefore 2.15 can be estimated by:

$$I(f, g) \geq e^{-\lambda_0 t} f_0 g_0 - e^{-\lambda_1 t} \|f\psi_X\|_2 \|g\psi_Y\|_2$$

By using the previous estimates and the fact that $\lambda_0 = 0$, we have:

$$\left(\int_X (f\psi_X)^2 \int_Y (g\psi_Y)^2 \right)^{\frac{1}{2}} e^{-\frac{D^2}{4t}} \geq f_0 g_0 e^{-\lambda_1 t} \|f\psi_X\|_2 \|g\psi_Y\|_2$$

Then:

$$e^{-\lambda_1 t} \|f\psi_X\|_2 \|g\psi_Y\|_2 \geq f_0 g_0 - \|f\psi_X\|_2 \|g\psi_Y\|_2 e^{-\frac{D^2}{4t}}$$

As the gaussian exponential has the property that can be made arbitrarily close to 0 by taking t enough small, we will choose t such that:

$$f_0 g_0 = 2 \|f\psi_X\|_2 \|g\psi_Y\|_2 e^{-\frac{D^2}{4t}}$$

Then:

$$\frac{-D^2}{4t} = \ln f_0 g_0 \|f\psi_X\|_2 \|g\psi_Y\|_2$$

and

$$t = \frac{D^2}{4 \ln \frac{2 \|f\psi_X\|_2 \|g\psi_Y\|_2}{f_0 g_0}}$$

. For this t we have:

$$e^{-\lambda_1 t} \|f\psi_X\|_2 \|g\psi_Y\|_2 \geq \frac{1}{2} f_0 g_0$$

which implies:

$$\lambda_1 \leq \frac{1}{t} \ln \frac{2\|f\psi_X\|_2\|g\psi_Y\|_2}{f_0g_0}$$

After substituting this value of t it follows that:

$$\lambda_1 \leq \frac{4}{D^2} \left(\ln \frac{2\|f\psi_X\|_2\|g\psi_Y\|_2}{f_0g_0} \right)^2$$

. It is important to underline that if either the manifold has not boundary or the Dirichlet or Neumann boundary condition is satisfied there is one eigenvalue $\lambda_0 = 0$ with the associated function being the constant function

$$\phi_0 = \frac{1}{\sqrt{v_g(M)}}.$$

Therefore we can choose $f = g = \phi_0$ and take into account that:

$$f_0 = \int_X f\phi_0 = \int_Y \phi_0^2$$

and

$$\|f\psi_X\|_2 = \left(\int_X \phi_0^2 \right)^{\frac{1}{2}} = \sqrt{f_0}$$

. Similar identities hold for g . We then obtain:

$$\lambda_1 \leq \frac{1}{D^2} \left(\ln \frac{4}{\int_X \phi_0^2 \int_Y \phi_0^2} \right)^2$$

Then, by substituting the value of ϕ_0 we have:

$$\begin{aligned} \lambda_1 &\leq \frac{1}{D^2} \left(\ln \frac{4}{\int_X \phi_0^2 \int_Y \phi_0^2} \right)^2 = \\ &\frac{1}{D^2} \left(\ln \frac{4}{\left(\frac{1}{v_g(M)}\right)^2 \int_X dv_g \int_Y dv_g} \right)^2 = \frac{1}{D^2} \left(\ln \frac{4(v_g(M)^2)}{v_g(X)v_g(Y)} \right)^2 \end{aligned}$$

Therefore:

$$\lambda_1 \leq \frac{1}{D^2} \left(1 + \ln \frac{(v_g(M)^2)}{v_g(X)v_g(Y)} \right)^2$$

. Now we consider the general case for $k > 2$. For a function $f(x)$, let f_i^j denote the i -th Fourier coefficient of the function $f\mathbf{1}_{X_j}$ i.e.

$$f_i^j = \int_{X_j} f\phi_i$$

. Similar to the case of $k = 2$, we have:

$$I_{lm}(f, f) = \int_{X_l} \int_{X_m} p(x, y, t) f(x) f(y) dv_g(x) dv_g(y)$$

. We have the following upper bound for $I_{lm}(f, f)$:

$$I_{lm}(f, f) \leq \|f\psi_{X_l}\|_2 \|g\psi_{Y_m}\|_2 \exp \frac{-D^2}{4t} \quad (2.16)$$

and the following lower bound:

$$I_{lm}(f, f) \geq e^{-\lambda_0 t} f_0^l f_0^m + \sum_{i=1}^{k-1} e^{-\lambda_i t} f_i^l f_i^m - e^{-\lambda_k t} \|f\psi_{X_l}\|_2 \|g\psi_{Y_m}\|_2 \quad (2.17)$$

The choice of appropriate l, m allows us to eliminate the term in the middle of the right-hand side of 2.16.

In fact if we consider $k + 1$ vectors $f^l = (f_1^l, \dots, f_{k-1}^l)$ in \mathbb{R}^{k-1} , with $l = 0, \dots, k$.

We endow this $k - 1$ dimensional space with a scalar product given by:

$$(v, w) = \sum_{i=1}^{k-1} v_i w_i e^{-\lambda_i t}$$

.

By using the previous corollary, out of any $k + 1$ vectors in $(k - 1)$ -dimensional Euclidean space, we always can find two vectors with non-negative scalar product. Hence there are different l, m such us $\langle f^l, f^m \rangle \geq 0$. Then:

$$\begin{aligned} I_{lm}(f, f) &\geq e^{-\lambda_0 t} f_0^l f_0^m + \sum_{i=1}^{k-1} e^{-\lambda_i t} f_i^l f_i^m - e^{-\lambda_k t} \|f\psi_{X_l}\|_2 \|g\psi_{Y_m}\|_2 \geq \\ I_{lm}(f, f) &\geq e^{-\lambda_0 t} f_0^l f_0^m - e^{-\lambda_k t} \|f\psi_{X_l}\|_2 \|g\psi_{Y_m}\|_2 \end{aligned} \quad (2.18)$$

Comparing 2.17 and 2.18 we have:

$$e^{-\lambda_k t} \|f\psi_{X_l}\|_2 \|g\psi_{Y_m}\|_2 \geq f_0^l f_0^m - \|f\psi_{X_l}\|_2 \|g\psi_{Y_m}\|_2 e^{\frac{-D^2}{4t}} \quad (2.19)$$

The rest of the proof is similar to the case $k = 2$. In fact we can choose t such that the right-hand side is at least $\frac{1}{2} f_0^l f_0^m$. We select:

$$t = \min_{l \neq m} \frac{D^2}{4 \ln \frac{2 \|f\psi_{X_l}\|_2 \|f\psi_{X_m}\|_2}{f_0^l f_0^m}}$$

. From 2.19, it follows:

$$\lambda_k \leq \frac{1}{t} \ln \frac{2\|f\psi_{X_t}\|_2\|f\psi_{X_m}\|_2}{f_0^l g_0^m}$$

. By substituting t from above and taking $f = \phi_0$, 2.14 follows. \square

It is important to underline that although differential geometry and spectral graph theory share a great deal in common, significant differences exist and depend on the fact that a graph is not "differentiable" and many geometrical techniques involving high-order derivatives are impossible to utilize for graphs. Moreover when it is possible to develop the discrete parallels, we have a different viewpoint that lead to an improvement of the original result from the continuous case.

Chapter 3

The Alzheimer's disease and other Dementias

3.1 Generalities about Dementia

Dementia is a category of brain diseases that cause mainly memory loss, inability to think and reason clearly and difficulties with activities of daily living. It is estimated to affect 25 million of people worldwide. Rarely the disease is diagnosed in people under 65 years of age, while 3 per cent of people between the ages of 65-74 have dementia and the percentage increases over the age of 85 with the 47 per cent of people affected.

The most common form of dementia is the Alzheimer's disease that was described for the first time in 1906 by a german psychiatrist and neuropathologist Aloise Alzheimer. The main symptoms concern cognitive impairment, psychiatric or behavioural disturbances and difficulty with activities of daily living. The course of the disease lasts more than 10 years and can be analyzed by identifying four stages: pre-dementia, early stage, moderate stage, advanced stage. The former is characterized by problems in remembering recent events or recently learned facts and inability to acquire new informations. This process is known as short term memory loss. These symptoms are often confused with "age-related" matters or manifestations of stress.

Therefore at the beginning the diagnosis of the AD is not immediate. In fact mild cognitive difficulties can be observed in patients up to eight years before they fulfil the clinical criteria for diagnosis of the disease. Other common symptoms deal with difficulties in the executive functions of attentiveness, planning, flexibility and abstract thinking, depression, irritability and apathy. The latter is the most persistent neuro-psychiatric symptom throughout the course of the AD.

It is important to underline that the preclinical stage of dementia is said in medical literature *mild cognitive impairment* (MCI). In fact the signs of the disease are subtle as they do not affect the person's daily functions. It is estimated that 70 per cent of those diagnosed with MCI will progress to dementia at some point.

The main feature of early stage of Alzheimer is the progressive impairment of memory and learning that leads to the definitive diagnosis. Memories capacities are not all affected in the same way. In fact increasing difficulties are observed in remembering recently-happened events and in learning new things, while long term memory (that includes autobiographical events happened in the past, learned facts and implicit memory i.e. the memory of the body on how to do things) is not seriously damaged. Language problems consist in an impoverishment of the vocabulary and in a decreased word fluency, but the person with Alzheimer's disease is able to express basic ideas adequately at this stage. Moreover he can perform many fine motor tasks like writing, drawing or dressing independently, but he may need assistance with the most cognitively activities, as the disease progresses.

In the moderate stage the subject affected by the disease becomes progressively unable to perform the most common activities of daily living. Coordination in complex motor sequences decreases with the consequent increase of the risk of falling. Reading and writing skills are seriously damaged until the complete loss. The impairment of speech fluency becomes significant and concerns typically the capacity to recall vocabulary with consequent incorrect word substitutions. The loss of the memory is severe at this stage as

also the long term memory is damaged and the person may fail to recognize close relative. Irritability, wandering, emotional lability and outbursts of unpremeditated aggression are often very common symptoms.

In the advanced stage the subject's dependence upon caregivers becomes complete, as he is unable to perform even the simplest task without any assistance. The loss of the memory and verbal language abilities is almost total. This leads the person to the death that is typically due to an external factor like an infection of pressure ulcers or pneumonia. In this sense AD is a terminal illness.

An other diffused form of dementia is Frontotemporal dementia (FTD). The

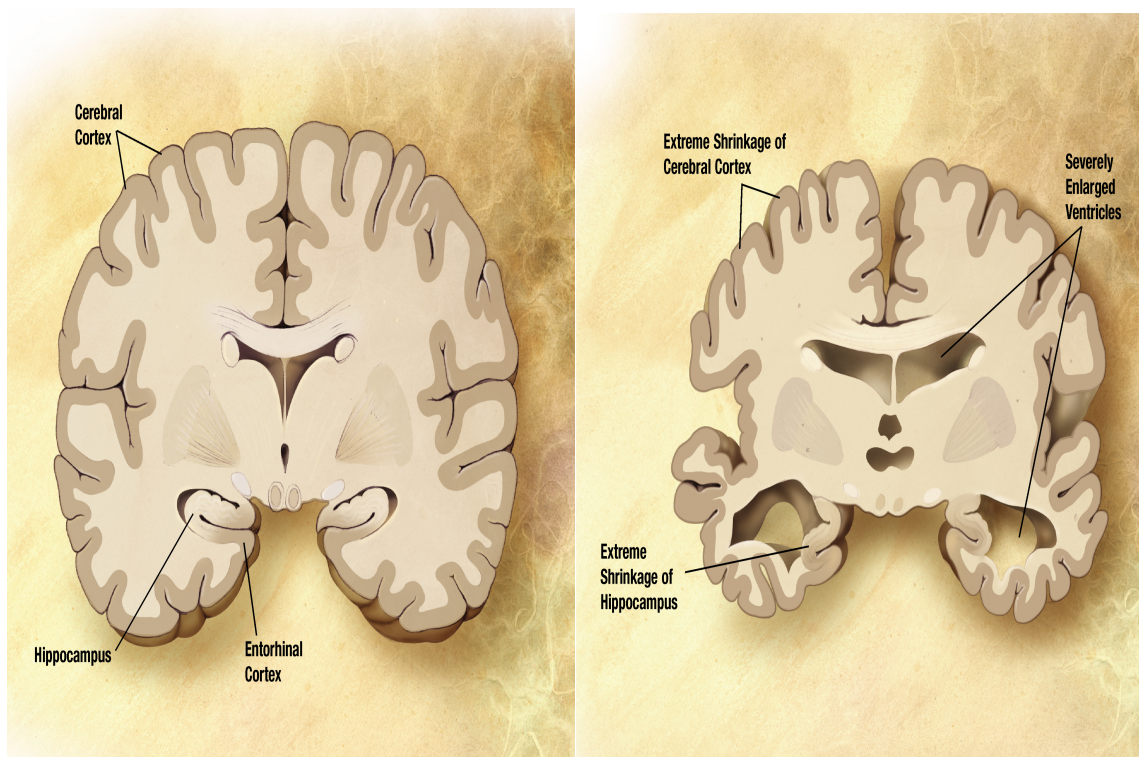


Figure 3.1: Comparison between an healthy brain and a brain affected by Alzheimer's disease

name is due to the fact that the degeneration i.e. the loss of neurons involves mainly the frontal and/or the temporal lobes. It affects almost equally men and women and the first signs of the disease manifest between the ages of 55

and 65. Symptoms are similar to those of Alzheimer's disease, as significant changes in social and personal behaviour, apathy, blunting of emotion and speech difficulties are observed. The latter is the most typical symptom of FTD and includes progressive loss of semantic understanding and difficulties in speech production. Unlike Alzheimer's disease memory does not appear seriously damaged. BvFTD stands for behavioural variant frontotemporal dementia and is characterized typically by changes in social behaviour and conduct, with loss of social awareness and poor impulse control. Other forms of dementia are Lewy body dementia, vascular dementia, corticobasal degeneration, normal pressure hydrocephalus and Creutzfeldt-Jakob disease.

The widespread of dementia leads many countries in the world to consider the care of people affected by it a national priority; therefore investments in cure research and in education to better inform social service workers, caregivers etc are significant.

Finally, it is important to underline the high social cost of dementia (especially in Europe and United States) that has been estimated to have reached 160 billion of dollars worldwide and includes direct medical cost such as nursing home care, direct non-medical cost such as in home day care and indirect cost such as the loss of productivity of both patient and caregiver.

3.2 Overview on findings about dementias' causes and progression mechanisms

The effective cause of Alzheimer's disease has not been identified yet and represents an open research challenge. Several significant hypotheses have been stated and are object of scientific research. Between them, we will focus on amyloid hypothesis and tau hypothesis. The former was elaborated in 1991. It is supported by the fact that amyloid precursor protein (APP) is localized on chromosome 21, together with the fact that people with trisomie 21 (Down Syndrome) who have an extra gene copy almost universally exhibit AD by 40 years of age. Moreover transgenic mice that express a

mutant form of human APP develop Alzheimer's-like brain pathology with spatial learning deficits.

Beta amyloid ($A\beta$ or Abeta) denotes peptides from 36 to 43 amino acids and represents the main component of the amyloid plaques found in the brains of Alzheimer patients. Beta amyloid originates from a larger protein called amyloid precursor protein (APP), a transmembrane protein that penetrates through the neuron's membrane. In Alzheimer's disease certain enzymes cut APP in "smaller fragments" that give rise to Beta amyloid. Fibrils of beta-amyloid produced by this process accumulate outside the neurons in dense formations known as senile plaques.

Tau hypothesis involves tau proteins that are abundant in neurons of the central nervous system. Every neuron has a cytoskeleton, an internal support structure partly made up of structures called microtubules. The latter act like tracks, guiding nutrients and molecules from the body of the cell to the ends of the axon and back. Tau protein stabilises the microtubules when phosphorylated, and is therefore called a microtubule-associated protein. In AD, as we will see later, tau undergoes chemical changes, becoming hyperphosphorylated; it then begins to pair with other threads of tau and create neurofibrillary tangles inside the nerve cell body. This process causes the disintegration of the microtubules and the collapse of neuron's transport system with the consequent malfunctions in biochemical communication between neurons and later the death of the cells.

Findings show that the mechanism underlying the formation of the beta amyloid plaques is based on the capacity of beta amyloid molecules to aggregate in several forms of flexible soluble oligomers(that is a molecular complex composed by a few monomers units). These oligomers can misfold, that is can change their structure assuming a pathological conformation, and walk throughout local and then long-range cerebral circuits via transsynaptic spread. Misfolded oligomers can induce other molecules of the same species to adopt the pathological form, triggering a chain reaction in which these misfolded proteins cascade along neuronal pathways. Tau protein shows a

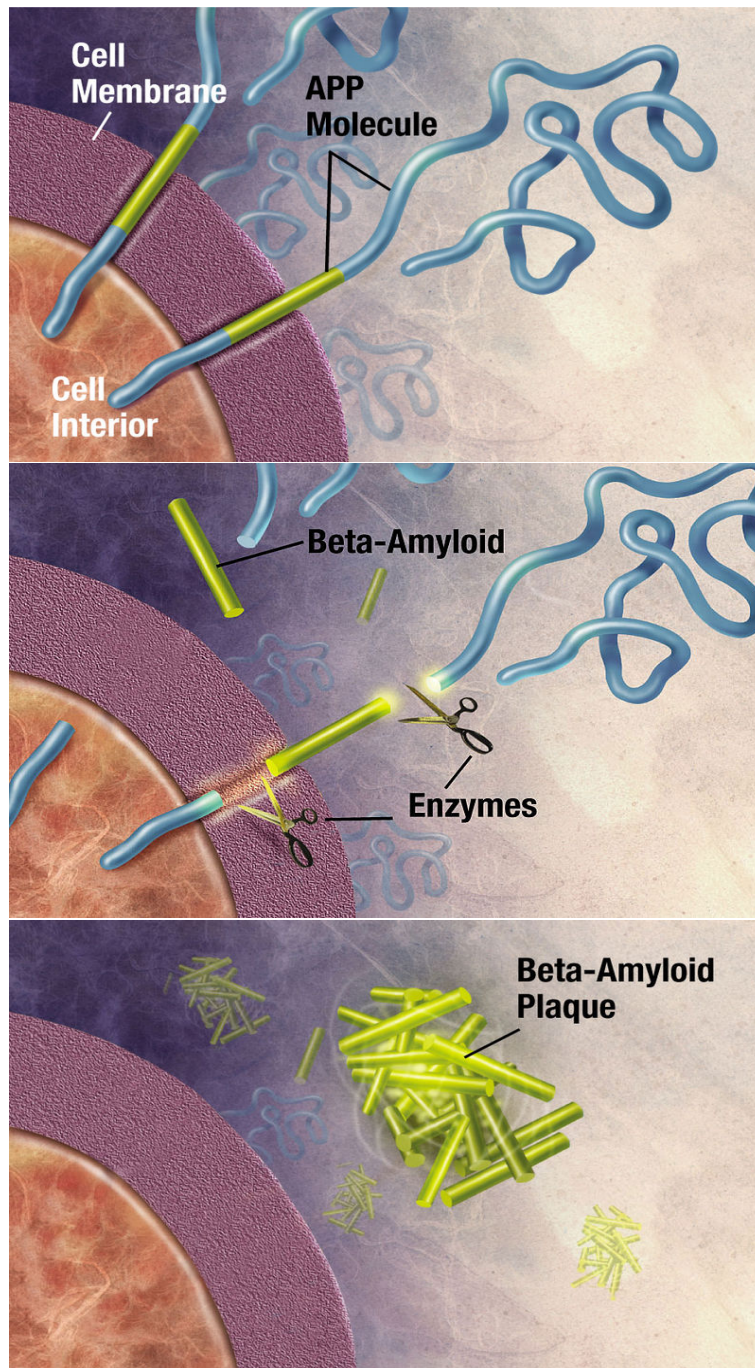


Figure 3.2: Formation of Beta-Amyloid plaques

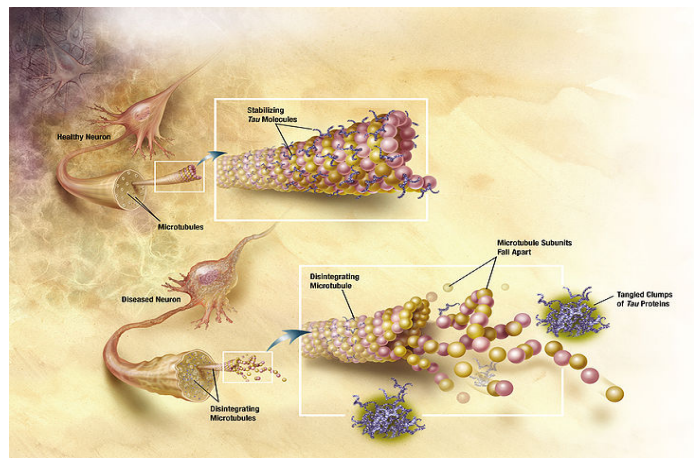


Figure 3.3: Disintegration of microtubules in brain cells due to misfolded tau protein

similar behaviour as it can form misfolded oligomers that propagate from the exterior to the interior of the cell and give rise to the misfolding of other tau oligomers with the consequent creation of neurofibrillary tangles. These mechanisms are also typical of other proteins like α -synuclein and TDP-43 involved in other dementias. Therefore the crucial observation is that all dementias seem to share a common mechanism of progression that seems similar to prions infections.

In fact, according to Prion Hypothesis, a prion is an infectious agent composed of protein in a misfolded form. It is made of PrP protein, that in its normal form (usually denoted by PrP^C is found in the body of healthy people and animals. A misfolded form of these protein, called PrP^{Sc} is responsible of a variety of diseases in mammals like, for example, bovine spongiform encephalopathy (BSE, also known as "mad cow disease"). When PrP^{Sc} penetrates an healthy cell , it acts like a template, inducing properly folded proteins to assume the disease-associated misfolded form.

Recent findings show that there is a relationship between Alzheimer's disease and PrP^C proteins. The latter appears involved in impairment of memory. More precicely, $A\beta$ oligomers are responsible of synaptic toxicity on neurons

with consequent damage of memory. It seems that this phenomenon is induced by a receptive membrane and the noxious agent involved is the PrP^C protein. Moreover prions proteins have been identified as APP-regulator, pointing out the strong link between them. This "prion-like" disease

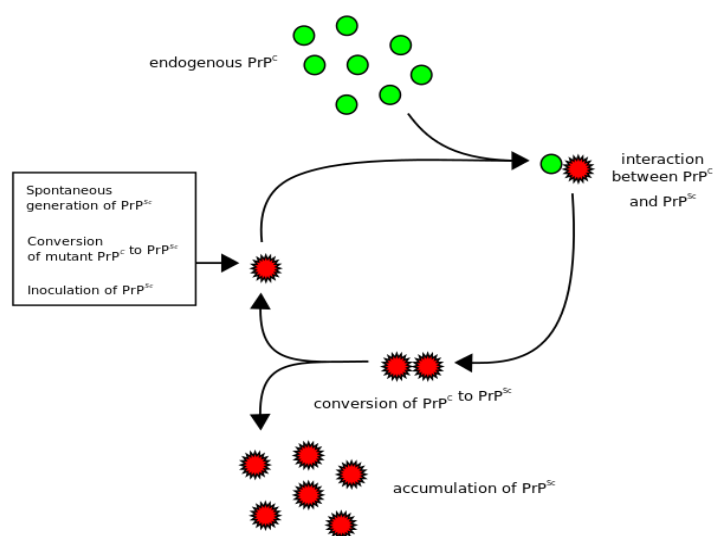


Figure 3.4: Heterodimer model of prion replication mechanism: a single PrP^{Sc} molecule binds to a single PrP^C molecule and catalyzes its conversion into PrP^{Sc} . The two PrP^{Sc} molecules then come apart and can go on to convert more PrP^C

progression strongly supports the hypothesis that the dementia's disease is transmitted along neuronal pathways. The latter comes from medical findings on neurodegeneration due to dementia.

Moreover, these studies show alterations in brain caused by neurodegeneration, that in the case of bvFTD only involve the orbitofrontal cortex, while in AD we have spatially distinct involvement of the posterior temporal heteromodal cortex due mainly to amyloid deposition. In conclusion, we can observe that various dementias selectively seem to affect distinct intrinsic brain areas, as these findings suggest.

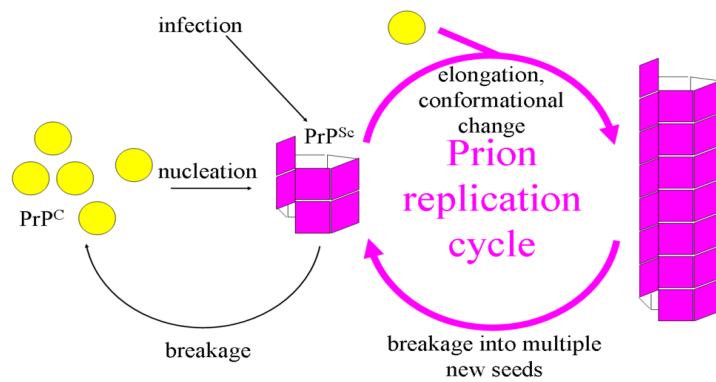


Figure 3.5: Fibril model of prion replication mechanism: it starts from the assumption that PrP^{Sc} exists only as fibrils. Fibril ends bind PrP^C and convert it into PrP^{Sc} .

Chapter 4

The Network Diffusion Model

4.1 Processing steps of the network diffusion model

In this section we will describe a model of progression of Alzheimer's disease (that can be applied also to all demantias since they are supposed to share a common progression mechanism by recent findings, as we saw in the previous chapter) which point of depart consists in the hypothesis of "prion-like" propagation of the disease and in its trasmission along neuronal pathways.

In fact the misfolded proteins responsible of the disease are supposed to "spread the pathological conformation" by inducing other proteins of the same type to adopt it. Recently misfolded proteins in turn infect other properly folded proteins; therefore the progression mechanism is diffusive and the number of infections at certain time increases according to the number of infection observed previously i.e. it depends on the concentration in regions of interest of the proteins involved in the process. In this view, in order to represent how this "prion-like" propagation takes place at microscopic level, we will introduce a "diffusion model" i.e. a classical model of random dispersion of a certain factor (that, in this case, it is a "disease factor") driven by concentration gradients . Moreover, each disease-causing agent (like ,for

example, tau-protein or beta-amyloid) characterized by rate of propagation along neuronal fibers proportional to concentration-levels differential of that disease agent is well modeled by diffusion speed.

The first step of this research consists in analyzing how "prion-like" propagation of the disease acts on the healthy brain, restricting this diffusive propagation to follow fiber pathways. Resulting macroscopic consequences and dynamics of this process are then mathematically derived.

In order to build a dataset which the analysis is based on, 14 young healthy volunteers have been undergone MRI of the brain, followed by the whole brain tractography of diffusion MRI scans. After that, specific areas of interest in brain have been identified, underlining the connections between them. In this way, "healthy brain network" is built. MRI scans of 18 AD, 18 bvFTD, 19 age-matched normal subjects are analyzed in order to identify patterns of disease. The "prion-like" propagation of disease in the "healthy brain network" is derived by mathematical approach, and finally theoretical results are compared with disease patterns experimentally obtained.

4.2 The network heat equation

In this section we will analyse by mathematical approach "how" the prion-like propagation of dementia acts on the healthy brain network. Therefore we will describe the Network Diffusion Model whose main feature consists in the approximation of the human brain with a finite weighted graph $G = \{V(G), E(G)\}$, in which the vertices $v_i \in V(G) = \{v_1, \dots, v_n\}$ represent the i th cortical or subcortical gray matter structure while the edges $e_{i,j}$ represent the connections by white-matter fiber pathways between structures i and j .

Moreover, we introduce a coefficient $c_{i,j}$ that is a measure of "how much" the structures i and j are connected. $c_{i,j}$ is said "weight" of the graph G . In this way we build a "brain network" in which the vertices v_i comes from the parcellation of brain MRI and $c_{i,j}$ is measured by fiber tractography.

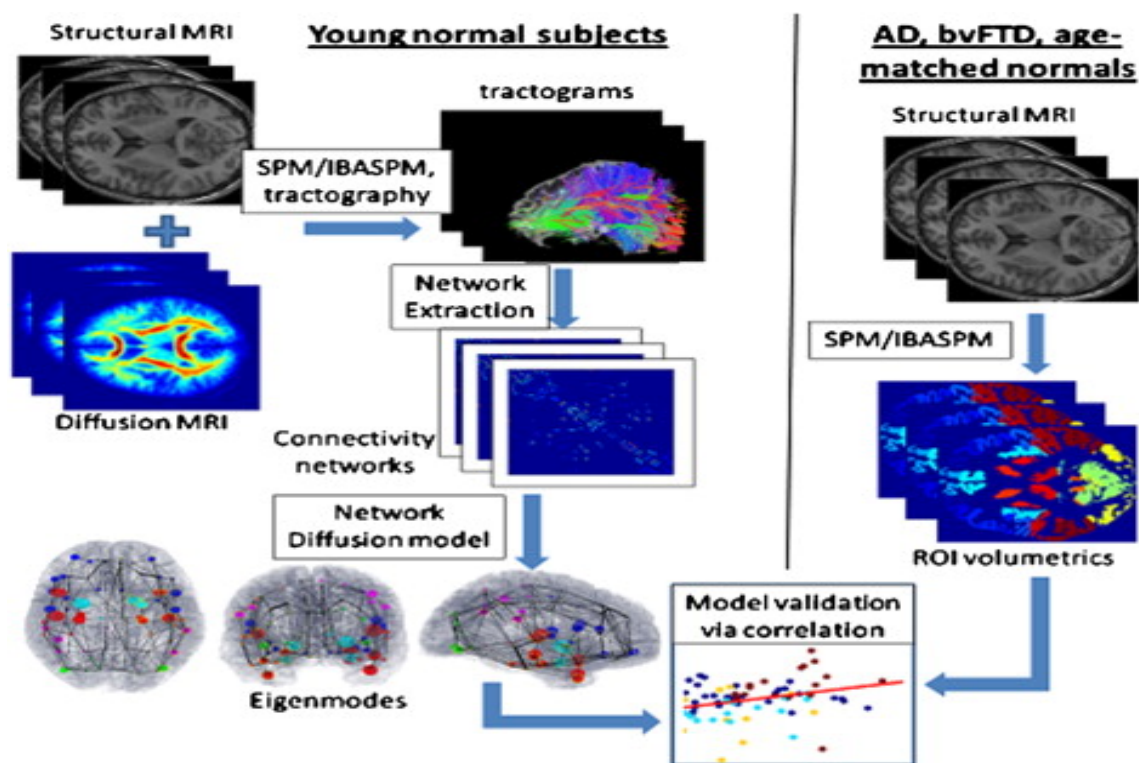


Figure 4.1: Diagram of the processing steps of the Network Diffusion Model: (left) "Healthy brain network" is obtained by MRI scans of 14 young volunteers followed by whole brain tractography. Cortical and subcortical gray matter regions are represented by nodes of the network, while the number and the strength of fiber tracts that connect them are described by the edges of the network. Proposed network diffusion model and its eigenmodes are derived from this healthy network. Predicted atrophy patterns are plotted. (right) Measurement of atrophy patterns of AD and bvFTD patients. Volume of each cortical and subcortical grey matter region is measured. Atrophy of each region is estimated through a statistic of interest between the diseased and the age-matched normal groups. The results are plotted and compared with predicted atrophy patterns.

In order to explain the development of the network diffusion model we consider a cerebral region R_2 affected by Alzheimer's disease and an unaffected cerebral region R_1 . We observe that to simplify we will talk about Alzheimer's disease, but results can be extended to all dementias. Conversely we introduce a function $X_2(t)$ that represents the concentration of the disease factor in the region R_2 at certain time $t \in \mathbb{R}^+$.

In the same way we define $X_1(t)$ for the region R_1 . We consider a time interval $[t, t + \delta t]$ and we set $X_2(t) = x_2$ and $X_1(\tau) = 0$, for $\tau < t$. We will analyze first the problem from microscopic point of view, describing the transmission of the Alzheimer disease through a diffusive process of the disease factor. The number of infections from region R_2 to R_1 at the time interval δt is given by $\beta c_{1,2} x_2 \delta t$, where $c_{1,2}$ represents the inter-region connection strength and $\beta > 0$ is the diffusivity constant that controls the propagation speed. Moreover we have a reverse diffusion of a certain quantity x_1 of the disease factor that is transmitted to R_2 (this is equivalent to affirm that at time t the disease factor in R_1 is given by $X_1(t) = x_1$). The number of infections from region R_1 to R_2 is $\beta c_{1,2} x_1 \delta t$.

Hence at time interval δt the concentration of the disease factor in R_1 ranges up to a quantity $\delta X_1 = X_1(t + \delta t) - X_1(t) = \beta c_{1,2} (x_2 - x_1) \delta t$. If we consider the limit $\delta t \rightarrow 0$ we have:

$$\frac{dX_1(t)}{dt} = \lim_{\delta t \rightarrow 0} \frac{X_1(t + \delta t) - X_1(t)}{\delta t} = \beta c_{1,2} (x_2 - x_1) \quad (4.1)$$

We will generalize 4.1 to the entire brain network (represented by the graph $G = \{V(G), E(G)\}$) using the laplacian of a weighted graph. To this aim, we will represent the disease factor at time t on the brain network by a vectorial function

$$x : V(G) \times \mathbb{R} \rightarrow \mathbb{R}^n$$

$$x(t) = x(\cdot, t) = \begin{pmatrix} x_1(v_1, t) \\ \vdots \\ x_n(v_n, t) \end{pmatrix}$$

in which the i th component $x_i(v_i, t)$ expresses the disease factor at time t on the vertex v_i . Let H be the following $n \times n$ matrix with real entries:

$$H_{i,j} = \begin{cases} \sum_{i,j': e_{i,j'} \in E(G)} c_{i,j'} & \text{if } i = j \\ -c_{i,j} & \text{if } v_i \text{ and } v_j \text{ are adjacent} \\ 0 & \text{otherwise} \end{cases} \quad (4.2)$$

From chapter one we know that the Laplacian of a weighted graph G is defined to be

$$\mathbf{H} = T^{-\frac{1}{2}} H T^{-\frac{1}{2}}$$

where T is the diagonal matrix with the (i, i) th entry having the value $d_{v_i} = \sum_{j=1}^n c_{i,j}$. Therefore \mathbf{H} is the following $n \times n$ matrix:

$$\mathbf{H}_{i,j} = \begin{cases} 1 - \frac{c_{i,i}}{d_{v_i}} & \text{if } i = j \\ \frac{-c_{i,j}}{\sqrt{d_{v_i} d_{v_j}}} & \text{if } v_i \text{ and } v_j \text{ are adjacent} \\ 0 & \text{otherwise} \end{cases} \quad (4.3)$$

Remark 8. As all brain region have not the same size, we normalize each row and column of 4.2 in order to obtain 4.3.

If we consider a time interval $[0, t] \subset \mathbb{R}$ and an initial data $x_0 = (x_0^1, \dots, x_0^n)$, we can generalize equation 4.1 by the following homogeneous system of linear differential equation:

$$\begin{aligned} \frac{dx(t)}{dt} &= -\beta \mathbf{H} x(t) \\ x(0) &= x_0 \end{aligned} \quad (4.4)$$

that is said "network heat equation".

Remark 9. It is important to underline that the initial data x_0 represents the initial pattern of the Alzheimer disease process.

From EDO theory we know that the solutions of 4.4 are of the form:

$$x(t) = \exp[-\beta \mathbf{H} t] x_0 \quad (4.5)$$

Remark 10. The term $\exp[-\beta \mathbf{H}t]$ is said "diffusion kernel" and acts like a spatial and temporal blurring operator. Equation 4.5 represents the "reaction" of the network in response to the propagation of the disease. Therefore it can be interpreted as the impulse response function of the network.

In order to calculate the diffusion Kernel we consider the following general results:

Definition 4.1. For an $n \times n$ matrix A we define $\exp[A]$ by:

$$\exp[A] = \sum_{h=0}^{\infty} \frac{A^h}{h!}$$

Lemma 4.2.1. *The following statements hold:*

1. (i) $\exp[0] = Id$
2. (ii) $\exp[A + B] = \exp[A] \exp[B]$, if $AB = BA$
3. (iii) $(\exp[A])^{-1} = \exp[-A]$
4. (iv) $\exp[CAC^{-1}] = C \exp[A]C^{-1}$, if $C \in GL(n, \mathbb{R})$ where $GL(n, \mathbb{R})$ is the set of all the invertible $n \times n$ matrices with entries in \mathbb{R} .

Proof. Statement (ii) follows from:

$$\begin{aligned} \exp[A + B] &= \sum_{h=0}^{\infty} \frac{(A + B)^h}{h!} = \sum_{h=0}^{\infty} \frac{1}{h!} \sum_{k=0}^h \binom{h}{k} A^k B^{h-k} = \\ &= \sum_{h=0}^{\infty} \sum_{k=0}^h \frac{A^k B^{h-k}}{k!(h-k)!} = \exp[A] \exp[B] \end{aligned}$$

by using $AB = BA$. Statements (i) and (iii) are directly consequences of (ii).

In order to prove statement (iv), we consider that:

$$(CAC^{-1})^h = CA(C^{-1}C)A(C^{-1} \dots C)AC^{-1} = CA^hC^{-1}$$

Hence by definition of exponential we have that:

$$\exp[CAC^{-1}] = \sum_{h=0}^{\infty} \frac{(CAC^{-1})^h}{h!} = \sum_{h=0}^{\infty} \frac{CA^hC^{-1}}{h!} =$$

$$= C \left(\sum_{h=0}^{\infty} \frac{A^h}{h!} \right) C^{-1} = C \exp[A] C^{-1}$$

□

Lemma 4.2.2. *Let A be a diagonal matrix:*

$$A = \text{diag}\{\lambda_1, \dots, \lambda_n\}$$

we have that:

$$\exp[A] = \text{diag}\{e^{\lambda_1}, \dots, e^{\lambda_n}\}$$

Proof. By using the fact that $A^h = \text{diag}\{\lambda_1^h, \dots, \lambda_n^h\}$ and by definition we have that:

$$\begin{aligned} \exp[A] &= \sum_{h=0}^{\infty} \frac{A^h}{h!} = \sum_{h=0}^{\infty} \frac{\text{diag}\{\lambda_1^h, \dots, \lambda_n^h\}}{h!} = \\ &= \text{diag}\left\{ \sum_{h=0}^{\infty} \frac{\lambda_1^h}{h!}, \dots, \sum_{h=0}^{\infty} \frac{\lambda_n^h}{h!} \right\} = \text{diag}\{e^{\lambda_1}, \dots, e^{\lambda_n}\} \end{aligned}$$

□

As the adjacency is a symmetric relation we have that our matrix \mathbf{H} is symmetric with entries in \mathbb{R} . This implies that its eigenvalues are real. Moreover we can apply *the spectral theorem* that affirms that we can decompose any symmetric matrix with real entries by using the *symmetric eigenvalue decomposition* (SED). This means that there exists an orthogonal matrix $U = [\mathbf{u}_1, \dots, \mathbf{u}_n]$ such that

$$H = U \Lambda U^T$$

where $\Lambda = \text{diag}\{\lambda_1, \dots, \lambda_n\}$. More precisely, \mathbf{u}_i is the eigenfunction for the eigenvalue λ_i , $i = 0, \dots, n$. Moreover the λ_i are given by equations 1.11, 1.12 and 1.13. By using the previous results, equation 4.5 becomes:

$$x(t) = \exp[-\mathbf{H}\beta t]x_0 = \exp[-U\Lambda U^T\beta t]x_0 = U \exp[-\Lambda\beta t]U^T x_0 =$$

$$\begin{aligned}
&= \begin{pmatrix} u_1^1 & u_2^1 & \dots & u_n^1 \\ \vdots & \vdots & \vdots & \vdots \\ u_1^n & u_2^n & \dots & u_n^n \end{pmatrix} \begin{pmatrix} e^{-\lambda_1 \beta t} & 0 & 0 & 0 \\ 0 & e^{-\lambda_2 \beta t} & 0 & 0 \\ \vdots & e^{-\lambda_i \beta t} & \vdots & \vdots \\ 0 & 0 & 0 & e^{-\lambda_n \beta t} \end{pmatrix} \begin{pmatrix} u_1^1 & u_2^1 & \dots & u_n^1 \\ \vdots & \vdots & \vdots & \vdots \\ u_1^n & u_2^n & \dots & u_n^n \end{pmatrix} \begin{pmatrix} x_0^1 \\ \vdots \\ x_0^n \end{pmatrix} = \\
&\begin{pmatrix} e^{-\lambda_1 \beta t} u_1^1 & e^{-\lambda_2 \beta t} u_2^1 & \dots & e^{-\lambda_n \beta t} u_n^1 \\ e^{-\lambda_1 \beta t} u_1^2 & e^{-\lambda_2 \beta t} u_2^2 & \dots & e^{-\lambda_n \beta t} u_n^2 \\ \vdots & \vdots & \vdots & \vdots \\ e^{-\lambda_1 \beta t} u_1^n & e^{-\lambda_2 \beta t} u_2^n & \dots & e^{-\lambda_n \beta t} u_n^n \end{pmatrix} \begin{pmatrix} u_1^1 & u_2^1 & \dots & u_n^1 \\ \vdots & \vdots & \vdots & \vdots \\ u_1^n & u_2^n & \dots & u_n^n \end{pmatrix} \begin{pmatrix} x_0^1 \\ \vdots \\ x_0^n \end{pmatrix} = \\
&\begin{pmatrix} \sum_j e^{-\lambda_j \beta t} u_j^1 u_j^1 & \sum_j e^{-\lambda_j \beta t} u_j^1 u_j^2 & \dots & \sum_j e^{-\lambda_j \beta t} u_j^1 u_j^n \\ \sum_j e^{-\lambda_j \beta t} u_j^2 u_j^1 & \sum_j e^{-\lambda_j \beta t} u_j^2 u_j^2 & \dots & \sum_j e^{-\lambda_j \beta t} u_j^2 u_j^n \\ \vdots & \vdots & \vdots & \vdots \\ \sum_j e^{-\lambda_j \beta t} u_j^n u_j^1 & \sum_j e^{-\lambda_j \beta t} u_j^n u_j^2 & \dots & \sum_j e^{-\lambda_j \beta t} u_j^n u_j^n \end{pmatrix} \begin{pmatrix} x_0^1 \\ \vdots \\ x_0^n \end{pmatrix} = \\
&\begin{pmatrix} \sum_i \sum_j e^{-\lambda_j \beta t} u_j^1 u_j^i x_0^i \\ \vdots \\ \sum_i \sum_j e^{-\lambda_j \beta t} u_j^n u_j^i x_0^i \end{pmatrix} = \begin{pmatrix} \sum_j e^{-\lambda_j \beta t} (\sum_i u_j^i x_0^i) u_j^1 \\ \vdots \\ \sum_j e^{-\lambda_j \beta t} (\sum_i u_j^i x_0^i) u_j^n \end{pmatrix} = \\
&= \begin{pmatrix} \sum_j e^{-\lambda_j \beta t} (\mathbf{u}_j^T x_0) u_j^1 \\ \vdots \\ \sum_j e^{-\lambda_j \beta t} (\mathbf{u}_j^T x_0) u_j^n \end{pmatrix} = \\
&= \sum_{j=1}^n (e^{-\beta \lambda_j t} \mathbf{u}_j^T x_0) \mathbf{u}_j \tag{4.6}
\end{aligned}$$

Remark 11. In the Network Diffusion Model the eigenfunctions of the Laplacian \mathbf{H} are said eigenmodes.

The eigenvalues of the Laplacian \mathbf{H} are in the interval $[0, 1]$ with a single $\lambda_1 = 0$ eigenvalue and a small number of near-zero eigenvalues. We observe that:

$$\lim_{t \rightarrow +\infty} e^{-\beta \lambda_i t} = 0$$

as $\beta > 0$, $\lambda_i \geq 0$ $i = 0, \dots, n$. The convergence speed depends on λ_i , i.e. the bigger λ_i is, more quickly the function converges to zero.

This means that, considering equation 4.6, most eigenmodes \mathbf{u}_i that correspond to larger eigenvalues decay quickly (that is for relatively small values of the variable t), leaving only the eigenmodes, that correspond to the smaller eigenvalues, to contribute.

The absolute values of the latter are said "persistent modes" and are the only eigenmodes significant in the progression of the Alzheimer disease.

4.3 Dynamics evolution of cortical atrophy

The main feature of the Alzheimer disease consists in the loss of neurons and synapsis in the cerebral cortex and in some subcortical regions, caused primarily by a plaque accumulation of abnormally folded beta-amyloid or tau amyloid proteins in the brain. Becoming structurally abnormal these proteins reduce the capacity of the neuron to trasmit the nerve impulse and cause the death of the neuron itself. In this sense the Alzheimer is said a misfolding protein disease. This process of "wasting away" of the affected regions of the brain is called "atrophy" and can be viewed like a measure of the level of progression of the Alzheimer disease. Moreover atrophy represents the most important mascroscopic consequence of disease propagation. We will talk about "cortical atrophy" because the process involves the cerebral cortex.

In this view, we are interested in studying the evolution of the atrophy in the time interval $[0, t]$. Therefore we make the hypothesis (on which this model is based) that cortical atrophy in k -th region of the brain is the accumulation of disease factor in k at time interval $[0, t]$. If we represent cortical atrophy in the k -th region (which in this model corresponds to the k -th vertex of the

network) by a function ϕ_k , we get the following equation:

$$\phi_k(t) = \int_0^t x_k(\tau) d\tau \quad (4.7)$$

Therefore on the whole brain we have:

$$\phi(t) = \int_0^t x(\tau) d\tau \quad (4.8)$$

From equation 4.6, we obtain:

$$\begin{aligned} \phi(t) &= \int_0^t x(\tau) d\tau = \int_0^t \sum_{i=1}^n (e^{-\beta\lambda_i\tau} \mathbf{u}_i^T x_0) \mathbf{u}_i d\tau = \\ &= \sum_{i=1}^n \int_0^t (e^{-\beta\lambda_i\tau} \mathbf{u}_i^T x_0) \mathbf{u}_i d\tau = \\ &= \sum_{i=1}^n \frac{-1}{\beta\lambda_i} [e^{-\beta\lambda_i\tau}]_0^t \mathbf{u}_i^T x_0 \mathbf{u}_i = \\ &= \sum_{i=1}^n \left(\frac{1 - e^{-\beta\lambda_i t}}{\beta\lambda_i} \right) \mathbf{u}_i^T x_0 \mathbf{u}_i \end{aligned} \quad (4.9)$$

We observe that cortical atrophy can be seen like the sum of atrophy relative to each eigenmode. Moreover for each eigenmode \mathbf{u}_i the corresponding atrophy increases with time and reaches its maximum in $\frac{1}{\beta\lambda_i} \mathbf{u}_i^T x_0 \mathbf{u}_i$. The time required to reach this quantity depends on λ_i and is bigger for the near zero eigenvalues. This means that lasting and significant contribute to the increase of atrophy i.e. to the progression of Alzheimer disease is observed only in the persistent modes. Moreover the slower is the decay rate, the more widespread and severe is the damage.

Remark 12. There is a significant relationship between the eigenvalues and the prevalence rates of the Alzheimer disease. The latter are calculated by comparing the number of people found to have the disease with the total number of people studied.

Therefore if the eigenmodes are good models of the Alzheimer disease and if we ignore genetic predisposition, population-wide prevalence rates should be

reflected by the rate of progression of the eigenmodes that are given by $\frac{1}{\lambda_i}$. We observe that prevalence rate are bigger for the near-zero eigenvalues. In this view, we can affirm that in the network diffusion model the persistent modes play a fundamental role in the progression of Alzheimer disease.

If we introduce a time varying externally driven disease process $\alpha(t)$ the dynamics of the system becomes:

$$x(t) = \int_0^t e^{-\beta \mathbf{H}t} x_0 \alpha(\tau) d(\tau) = (e^{-\beta \mathbf{H}t} x_0 * \alpha)(t) = \sum_{i=0}^n (e^{-\beta \lambda_i t} * \alpha)(t) \mathbf{u}_i \mathbf{u}_i^T \quad (4.10)$$

The meaning of equation 4.10 is that the behaviour of the disease dynamics can be controlled by a small number of distinct eigenmodes also in the case of an unknown external attack process.

Therefore the patho-physiological nature, location and frequency of neurodegenerative attack can be ignored in this model.

4.4 The role of the eigenmodes in Network Diffusion Model

In the previous section we derived the "eigenmodes" i.e. the eigenfunctions of the laplacian \mathbf{H} of the weighted graph G that represents the brain network. We showed that the disease factor at time t , $x(t)$ and the corresponding atrophy function $\phi(t)$ can be written in terms of these eigenmodes. Moreover, we saw that only a few number of eigenvalues is significant in the progression of disease.

Therefore its corresponding eigenfunctions, that we call "persistent modes" are the only one that determine atrophy patterns in this model. These considerations suggest that there is a strong correspondence between the healthy network's eigenmodes, that can be seen as spatial distinct patterns, and atrophy patterns of normal aging and dementia. Moreover, this statement is

also consistent with findings showing as various dementias selectively target distinct intrinsic brain regions. As the eigenfunctions of the Laplacian of a graph are functions on the set of the vertices of the graph, the eigenfunctions significant for the progression of atrophy are calculated and their values on each vertex of the network are compared (as it is shown in figures 4.2, 4.3, 4.4) with the amount of atrophy measured for each form of dementia (considered in the dataset) in the cerebral area corresponding to that vertex. Strong correspondence is observed between theoretical and experimental results. In fact, the first eigenmode that corresponds to the eigenvalue $\lambda_1 = 0$ varies simply according to region size, in strong resemblance with atrophy seen in normal aging. The second most persistent mode is a good representation of Alzheimer's atrophy in mesial posterior cingulate, limbic structures, lateral temporal and dorsolateral frontal cortex. The most involved areas by this eigenmode are the medial and lateral temporal lobe and the dorsolateral prefrontal cortex that are respectively implicated in memory and working memory. The third eigenmode closely resembles bvFTD atrophy patterns that typically involve orbitofrontal and anterior cingulate regions, as shown by recent findings. Brain regions where this eigenmode is particularly strong are the lateral temporal lobe and the superior frontal, dorsolateral orbital cortices. The latter deals with decision making, balancing risk versus reward and inhibition. Its degeneration can cause disinhibited behaviour, that is the main symptom of bvFTD.

We have affirmed in several occasions that the Network Diffusion Model is based on the hypothesis of prion-like diffusion of the disease. Therefore if dementias share this concentration-dependent diffusive mechanism that can reproduce atrophy patterns, we are allowed to consider the possibility that although etiologically distinct, the various dementias have common macroscopic consequences. In fact the model considers a generalized "disease factor" without differentiate among its origins or causes. This is justified, considering that the specific biochemical properties of the prion-like agent may be inconsequential for the macroscopic manifestation of disease. For exam-

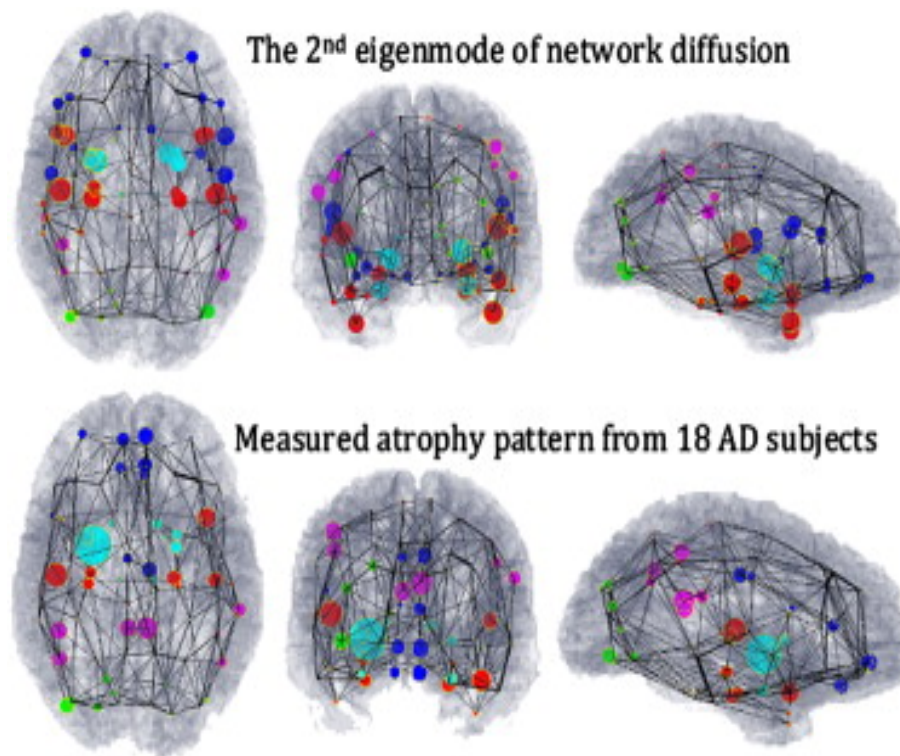


Figure 4.2: Visual correspondence between theoretical prediction and measured Alzheimer's atrophy patterns: Wire-and-ball plot represent whole brain atrophy patterns, where each brain region of interest is depicted as a ball whose size is proportional to the atrophy level in that area. The color of the ball denotes the lobe of interest: blues stands for frontal lobe, purple parietal lobe, green occipital lobe, red temporal lobe and cyan subcortical region. (Top) Theoretical prediction of atrophy is based on the second eigenmode of the young healthy brain network's Laplacian matrix H . The second eigenmode evaluated at each region of interest is represented by the size of the corresponding ball. (Bottom) Measured atrophy patterns obtained by 18 AD patients are represented. We observe strong correspondence between predicted and measured atrophy.

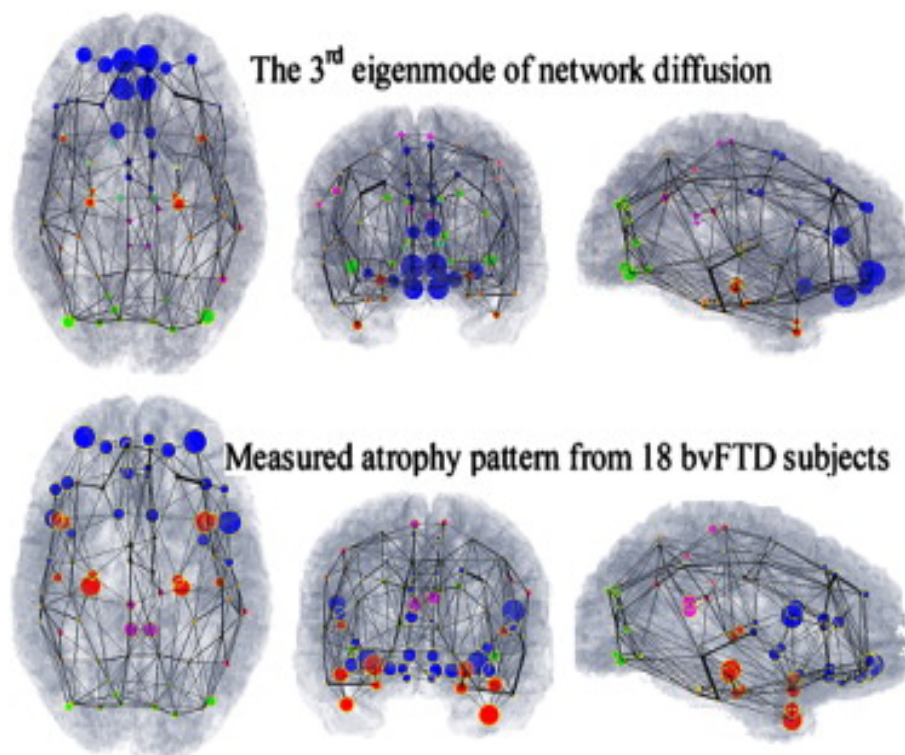


Figure 4.3: Visual correspondence between theoretical prediction and measured bvFTD's atrophy patterns:(Top) Theoretical prediction of atrophy is based on the third eigenmode of the young healthy brain network's Laplacian matrix H . The value of the third eigenmode at each region of interest is represented by the size of the corresponding ball.(Bottom) Atrophy patterns measured in brain region of interest obtained by 18 bvFTD patients are represented by the size of the corresponding ball. We observe strong resemblance between predicted and measured atrophy.

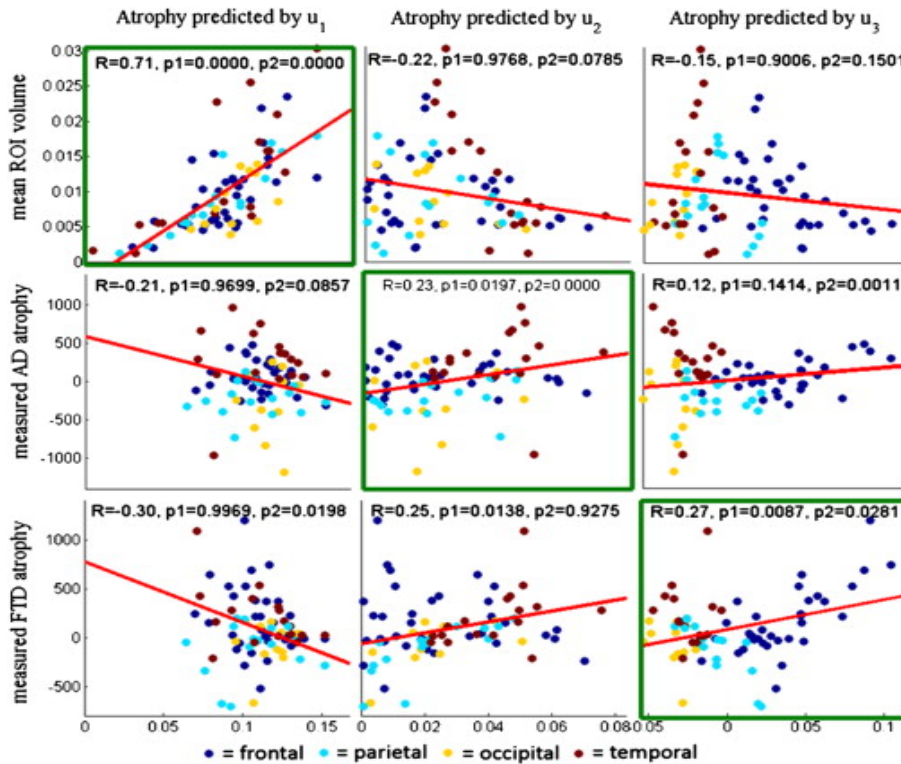


Figure 4.4: Correlations between Measured Atrophy of AD/bvFTD versus Predicted Atrophy from the First Three Eigenmodes of the Young Healthy Network: The x axis in each panel represents a measured level of atrophy through a statistic of interest (bottom). The y axes are eigenmodes of the healthy network: u_1 (left column), u_2 (middle column), and u_3 (right column). Each dot in the plots corresponds to a single grey matter region. Different colors of dots stand for different lobes. A line of best fit is also shown in each panel. Correlations within diagonally located panels are high, and correlations in off-diagonal panels are low. Most significant plots are indicated by green boxes, and they are along the diagonal panels. High correspondence between eigenmodes and dementia atrophy is shown.

ple, the spatial distribution of beta amyloid pathology in AD is not well correlated with whole brain atrophy patterns , while tau is well-correlated. However, neither tau nor beta amyloid are specific to AD and are found in semantic dementia or frontotemporal lobar degeneration (FTLD) subtype. These results show that clinical presentation of dementias depends only on the brain regions they affect and this agree with what proposed by network diffusion model, as the macroscopic consequences of disease progression are presented without analyzing the "disease factor" in its specific.

The main contribution of the model is that it turns qualitative understanding of disease's transmission into a quantitative model and provides a plausible alternative explanation for the apparent selective vulnerability of brain regions in various dementias.

4.5 Medical and diagnostic implications of the model

Patterns of dementia obtained by Network Diffusion Model agree with patterns of demetia provided on analysis on affected patients. Moreover in this model there is not any dependence on the brain region affected or in which the disease originates, as its point of depart consists in the statement that although the various dementias have different causes and produce different effects due to brain degeneration, they are supposed to share a common mechanism of progression. Conclusions of the model do not depend on inter-subjects variability or on instruments used to build the network and finally the model underlines the strong link existing between age and dementia. Consequences of these findings are significant from a medical point of view, as thanks to the strong correspondence between atrophy and eigenvalues future radiologists instead of analyse high dimensional and more complex whole brain atropy, may look only at the contribution the first three eigenmodes. Therefore they will deal with a simpler problems.

Another important consequence of this model is that it allows to predict

decline. In fact, starting from equation 4.1 and MRI of the patient, future patterns of atropy can be predicted. Knowledge of what the future holds allows prevention and informed choices regarding lifestyle.

Chapter 5

Appendix

5.1 The calculus of the exponential matrix

Theorem 5.1.1. *Let A be a $n \times n$ matrix, the $\exp[tA]$ is calculated by the following formula*

$$\exp[tA] = \sum_{i=1}^k e^{\lambda_i t} \left[I_n + \sum_{h=1}^{n-1} \frac{t^h}{h!} N^h \right] P_i(A) \quad (5.1)$$

where λ_i $i = 1, \dots, k$ are the distinct eigenvalues of A , N is a nilpotent matrix that follows from the S-N decomposition of A and $P_i(A)$ are projection matrices.

Remark 13. We define the projection $P_i(A)$ in the following way: let λ_i $i = 1, \dots, k$ be the distinct eigenvalues of A , m_i their respective multiplicities and $p_A(\lambda) = (\lambda - \lambda_1)^{m_1} (\lambda - \lambda_2)^{m_2} \dots (\lambda - \lambda_k)^{m_k}$ the characteristic polynomial of A . We can decompose $\frac{1}{p_A(\lambda)}$ into partial fraction $\frac{1}{p_A(\lambda)} = \sum_{i=1}^k \frac{Q_i(\lambda)}{(\lambda - \lambda_i)^{m_i}}$ where for every i the quantity Q_i is a non zero polynomial in λ of degree not greater than m_{i-1} . Therefore

$$1 = \sum_{i=1}^k Q_i(\lambda) \prod_{h \neq i} (\lambda - \lambda_h)^{m_h} \quad (5.2)$$

. We set

$$P_i(\lambda) = Q_i(\lambda) \prod_{h \neq i} (\lambda - \lambda_h)^{m_h} \quad (5.3)$$

Hence we define the projection by:

$$P_i(A) = Q_i(A) \prod_{h \neq i} (A - \lambda_h I_n)^{m_h} \quad (5.4)$$

We note that from 5.2 and 5.3 it follows:

$$1 = \sum_{i=1}^k P_i(\lambda)$$

and from 5.4

$$I_n = \sum_{i=1}^k P_i(A)$$

Before proving the theorem, we enunciate an other useful result:

Theorem 5.1.2. *Let A be an $n \times n$ matrix with complex entries. Then there exist two $n \times n$ matrices S , N (where S stands for symmetric matrix) such that:*

1. S is diagonalizable
2. N is nilpotent
3. $A = S + N$
4. $SN = NS$

Moreover the two matrices are uniquely determined by these four conditions and if A is real, also N and S are real.

Proof. We prove first the existence of S and N . We define S by

$$S = \lambda_1 P_1(A) + \lambda_2 P_2(A) + \dots + \lambda_k P_k(A)$$

where where λ_i $i = 1, \dots, k$ are the distinct eigenvalues of A , $P_i(A)$ are projection matrices. We consider the linear map

$$P_i(A) : \mathbb{C}^n \rightarrow \mathbb{C}^n$$

$$q \rightarrow P_i(A)q$$

and we denote by V_i its image. We observe that a vector $p \in V_i$ if and only if $P_i(A)q = p$ for some $q \in \mathbb{C}^n$. Therefore we have:

$$P_i(A)p = P_i(A)^2q = P_i(A)q = p$$

by projections propriety. Let n_i be the dimension of the space V_i over \mathbb{C} and let $p_{i,l} : l = 1, \dots, n_i$ be a basis for V_i . Then there exists an $n_i \times n_i$ matrix such that

$$(A - \lambda_i I_n)[p_{i,1}, p_{i,2}, \dots, p_{i,n_i}] = [p_{i,1}, p_{i,2}, \dots, p_{i,n_i}]N_i$$

as the coordinate-wise representation relative to this basis. By the previous observation this implies that:

$$\begin{aligned} (A - \lambda_i I_n)^l P_i(A)[p_{i,1}, p_{i,2}, \dots, p_{i,n_i}] &= (A - \lambda_i I_n)^l [p_{i,1}, p_{i,2}, \dots, p_{i,n_i}] = \\ &= [p_{i,1}, p_{i,2}, \dots, p_{i,n_i}]N_i^l \end{aligned}$$

for $l \in \mathbb{N}_0$. By projections propriety we have that $(A - \lambda_i I_n)^{m_i} P_i(A) = 0$; this implies $[p_{i,1}, p_{i,2}, \dots, p_{i,n_i}]N_i^{m_i} = 0$ and therefore $N_i^{m_i} = 0$. Hence N_i is a nilpotent matrix. Thus we obtain:

$$A[p_{i,1}, p_{i,2}, \dots, p_{i,n_i}] = [p_{i,1}, p_{i,2}, \dots, p_{i,n_i}](\lambda_i I_n + N_i)$$

Let $\{\mathbf{p}_{j,l}, l = 1, \dots, n_j\}$ be a basis for $V_j, j = 1, \dots, k$. Set

$$P_0 = [\mathbf{p}_{1,1}, \dots, \mathbf{p}_{1,n_1}, \mathbf{p}_{2,1}, \dots, \mathbf{p}_{2,n_2}, \dots, \mathbf{p}_{k,1}, \dots, \mathbf{p}_{k,n_k}] \quad (5.5)$$

. Then $P_0 \in GL(n)$ and we have that:

$$P_0^{-1}AP_0 = \text{diag}[\lambda_1 I_1 + N_1, \lambda_2 I_2 + N_2, \dots, \lambda_k I_k + N_k] \quad (5.6)$$

Therefore, we define:

$$S = \lambda_1 P_1(A) + \lambda_2 P_2(A) + \dots + \lambda_k P_k(A)$$

and $N = A - S$. By expression 5.5, we have that:

$$P_0^{-1}SP_0 = \text{diag}[\lambda_1 I_1, \lambda_2 I_2, \dots, \lambda_k I_k]$$

and

$$P_0^{-1}NP_0 = \text{diag}[N_1, N_2, \dots, N_k]$$

. Hence S is diagonalizable and N is nilpotent. Moreover $NS = SN$ as N and S are polynomials in A .

The existence of N and S satisfying items i, ii, iii, iv is shown. In order to prove the uniqueness, we consider an other pair (\bar{N}, \bar{S}) of $n \times n$ matrices satisfying items i, ii, iii, iv. Then iii and iv imply that $\bar{S}A = A\bar{S}$ and $\bar{N}A = A\bar{N}$. Hence $\bar{S}S = S\bar{S}$, $\bar{N}N = N\bar{N}$, $N\bar{S} = \bar{S}N$ and $S\bar{N} = \bar{N}S$ since S and N are polynomials in A . This implies that $S - \bar{S}$ is diagonalizable and $N - \bar{N}$ is nilpotent. Therefore, from $S - \bar{S} = N - \bar{N}$, it follows that $S - \bar{S} = N - \bar{N} = O$. \square

We are ready to prove theorem 5.1.1

Proof. Let $P_j(A)$ $j = 1, \dots, k$ be the projections defined as in 5.4. By using the previous theorem we have:

$$\begin{aligned} I_n &= \sum_{i=1}^k P_j(A) \\ S &= \sum_{i=1}^k \lambda_j P_j(A) \\ N &= A - S \end{aligned}$$

and

$$P_j(A)P_i(A) = \begin{cases} P_j(A) & \text{if } i = j \\ 0 & \text{if } i \neq j \end{cases}$$

Matrices N and M commutes.

Let V_j be the image of the map $P_j(A) : \mathbb{C}^n \rightarrow \mathbb{C}^n$. It is known that $S\mathbf{p} = \lambda_j\mathbf{p}$ for $\mathbf{p} \in V_j$. It follows that $S^l\mathbf{p} = \lambda_j^l\mathbf{p}$. Therefore:

$$\begin{aligned} \exp[tS]\mathbf{p} &= \left\{ 1 + \sum_{h=1}^{\infty} \frac{(\lambda_j t)^h}{h!} \right\} \mathbf{p} = \\ &= e^{\lambda_j t} \mathbf{p} \end{aligned}$$

5.2 The structure of solutions of homogeneous linear systems of EDO

and

$$\exp[tN] = I_n + \sum_{h=1}^{n-1} \frac{N^h t^h}{h!}$$

since N is nilpotent. Hence:

$$\begin{aligned} \exp[tA]\mathbf{p} &= \exp[tS + tN]\mathbf{p} = \exp[tS] \exp[tN]\mathbf{p} = \\ &= e^{\lambda_j t} \exp[tN]\mathbf{p} = \\ &= e^{\lambda_j t} \left[I_n + \sum_{h=1}^{n-1} \frac{N^h t^h}{h!} \right] \mathbf{p} \end{aligned} \quad (5.7)$$

for $p \in V_j$.

Applying 5.7 to a general $\mathbf{p} \in \mathbb{C}^n$, we obtain:

$$\exp[tA] = \sum_{j=1}^k e^{\lambda_j t} \left[I_n + \sum_{h=1}^{n-1} \frac{N^h t^h}{h!} \right] \mathbf{p} \quad (5.8)$$

for $\mathbf{p} \in \mathbb{C}^n$ and the proof is complete. \square

5.2 The structure of solutions of homogeneous linear systems of EDO

In this section we will analyze some basic results concerning the structure of solutions of homogeneous linear systems of linear differential equations given by:

$$\frac{dy}{dt} = A(t)y \quad (5.9)$$

where the entries of the $n \times n$ matrix A are continuous on an interval $I = \{a \leq t \leq b\}$.

Theorem 5.2.1. *The solutions of 5.9 form an n -dimensional vector space on \mathbb{C} .*

Proof. The proof is divided in three observations:

- Observation I:

Any linear combination of a finite number of solutions of 5.9 is a solution of 5.9. Moreover each column vector of a solution Y of the differential equation

$$\frac{dY}{dt} = A(t)Y \quad (5.10)$$

on an $n \times n$ unknown matrix Y is a solution of system 5.9. Therefore constructing an invertible solution Y of 5.10 we can construct n linearly independent solutions of 5.9. If an $n \times n$ matrix $Y(t)$ is a solution of 5.10 on an interval $I = \{a \leq t \leq b\}$ and $Y(t) \in GL(n) \forall t \in I$, then it is called fundamental matrix of solutions of 5.9 on I . Moreover n columns of a fundamental matrix of solutions of 5.10 form a fundamental set of n linearly independent solutions of 5.9 on interval I .

- Observation II:

Let $\phi(t)$ be a solution of 5.10 on I . Also, let $\psi(t)$ be a solution of the adjoint equation

$$\frac{dZ}{dt} = -A(t)Z \quad (5.11)$$

on the interval I where Z is an unknown matrix. Then

$$\frac{d}{dt} [\psi(t)\phi(t)] = -\psi(t)A(t)\phi(t) + -\psi(t)A(t)\phi(t) = 0$$

This implies that the matrix $\psi(t)\phi(t)$ is independent of t . Therefore, $\psi(t)\phi(t) = \psi(\tau)\phi(\tau)$ for any fixed point $\tau \in I$ and for all $t \in I$. In particular in the case when $\phi(\tau) \in GL(n)$ by choosing $\psi(\tau) = \phi^{-1}(\tau)$, we obtain $\psi(t)\phi(t) = I_n$ for all $t \in I$.

- Observation III:

Denote by $\phi(t, \tau)$ the unique solution of the initial value problems:

$$\frac{dY}{dt} = A(t)Y \quad Y(\tau) = I_n \quad (5.12)$$

where $\tau \in I$. Then $\phi(t, \tau) \in GL(n)$ for all t and the general structure of solutions is given by the following theorem, whose corollary is the theorem that we are proving.

5.2 The structure of solutions of homogeneous linear systems of EDO

Theorem 5.2.2. *The \mathbb{C}^n valued function $y(t) = \phi(t, \tau)\eta$ is the unique solution of the initial value problem*

$$\frac{dy}{dt} = A(t)y \quad y(\tau) = \eta$$

where $\eta \in \mathbb{C}^n$, while the $n \times n$ matrix $Y = \phi(t, \tau)\Gamma$ is the unique solution of the initial value problem

$$\frac{dY}{dt} = A(t)Y \quad Y(\tau) = \Gamma$$

where $\Gamma \in M_n(\mathbb{C})$

□

Remark 14.

- The general form of a fundamental matrix of solutions of 5.9 is given by $Y = \phi(t, \tau)\Gamma$ where $\Gamma \in GL(n)$
- If a fundamental matrix of solutions is given by $Y(t) = \phi(t, \tau)\Gamma$, then $Y(\tau) = \Gamma$. Hence

$$\phi(t, \tau) = Y(t)Y(\tau)^{-1}$$

for any fundamental matrix solution $Y(t)$. In particular

$$\phi(t, \tau) = \phi(t, \tau_1)\phi(t, \tau_1)^{-1}$$

for $t, \tau, \tau_1 \in I$

- The solutions of the differential equation

$$\frac{dy}{dt} = Ay \tag{5.13}$$

where A is a matrix with constant coefficients are given by 5.8.

Bibliography

- [1] Fan R. K. Chung, *Spectral Graph Theory*, American Mathematical Society, Providence, Rhode Island
- [2] Bela Bollobas, *Modern Graph Theory*, Springer, 1998
- [3] Ashish Ray, Amy Kuceyeski, Michael Weiner *A Network Diffusion Model of Disease Progression in Dementia*, Neuron, 2012
- [4] Kumar V., Abbas A.K., Fausto N., Aster J.C. Robbins e Cotran *Le basi patologiche delle malattie-Patologia generale* VIII edizione, Volume 2
- [5] Po-Fang Hsieh, Yasutaka Sibuya, *Basic Theory of Ordinary Differential Equations*, Springer
- [6] Edoardo Sernesi *Geometria I*, Bollati Boringhieri
- [7] "About Alzheimer's Disease: Symptoms" National Institute on Aging, retrieved on 28 December 2011
- [8] Polvikoski T, Sulkava R, Haltia M, Kainulainen K, Vuorio A, Verkkoniemi A, Niinistö L, Halonen P, Kontula K, *Apolipoprotein E, Dementia, and Cortical Deposition of Beta-amyloid Protein* The New England Journal of Medicine, 1995
- [9] Kramer JH, Jurik J, Sha SJ et al. (December 2003). *Distinctive neuropsychological patterns in frontotemporal dementia, semantic dementia, and Alzheimer disease*, Cogn Behav Neurol, 2008

Ringraziamenti

Ringrazio di cuore il prof. Bruno Franchi per la disponibilità, la gentilezza, la saggezza, l'intelligenza e l'apertura mentale di chi crede nel proprio lavoro. Lo ringrazio, inoltre, per avermi dato fiducia e per il prezioso sostegno fornitomi per la redazione di questa tesi.

Ringrazio il prof. Mirko Degli Esposti per aver gentilmente letto la tesi e espresso il suo interesse circa gli argomenti trattati.

Ringrazio Giulia e il suo occhio acuto di chi sa guardare il mondo senza giudizio per la sua capacità di accogliere, per avermi fatto scoprire un nuovo mondo aprendomi una nuova prospettiva, un nuovo punto di vista che io non credevo possibile; per avermi aiutato a trovarmi e ritrovarmi quando le mie energie venivano meno.

Un pensiero speciale va alle mie care amiche di "viaggio", ovvero all'energia e entusiasmo di Valentina, alla dolcezza di Chiara M., al sostegno di Chiara e al problem-solving di Giulia.

Ringrazio Gennaro e Giovanna, mie prime guide tra i portici di Bologna, quando tutto per me in questa città era ancora nuovo e sconosciuto.

Ringrazio Davide per avermi incoraggiato in un lontano momento buio.

Ringrazio la mia compagna di corso ed ex coinquilina Chiara Nard., per tutte le giornate di studio passate insieme sognando di scoprire gli spazi N-T, per le brillanti filosofie, e per le avventure in cui ci lanciavamo nella scoperta dell'animata vita bolognese.

Ringrazio la mia amica romana e compagna di corso della triennale Claudia per la sua lunga amicizia o meglio per essere rimaste comunque amiche, an-

che se spesso attualmente a distanza.

Ringrazio i miei nuovi coinquilini Giada, Enrico e Luca per il meraviglioso clima familiare che si è creato e, su suggerimento di Enrico, ringrazio il mio divano, per essere stato un fedele e comodo alleato durante la scrittura di questa tesi.

Ringrazio tutti i miei compagni di corso, i miei amici "bolognesi" e "teatranti": Camilla, Silvia, Romolo, Alice e il loro spirito di vino, Marta, Yesica, Paola, Paulo, Giannino e il suo animo sudamericano, Beppe, Chiara Micol (che in realtà è romana) e la sua ironicissima filosofia di vita, Silvia, Giulia, Giacomo, Michela, Daniele, Enzo, Francesca, Alex, Marco, le "belle Else" ovvero Ilaria, Lara, Elisa, Carlotta, Federica e Annalisa per le felici serate passate insieme e per aver reso così belli e indimenticabili i miei anni universitari a Bologna. Ringrazio la gentilissima e professionalissima Alice Barbieri, per essere sempre di grande aiuto e dalla parte degli studenti.

Ringrazio i miei amici erasmus "madrileni": Michele, Giada, Sarah, Marielle, Tabea, la Greciana e Maria Ines per l'allegria, il confronto culturale e i bei momenti trascorsi in terra ispanica. Ringrazio i vicoli e i portici di Bologna, luogo di a volte solitarie e lunghe passeggiate, e le loro bellissime luci, e gli scorci inaspettati.

Ringrazio mia mamma, mio padre e la mia piccola sorella Valeria.